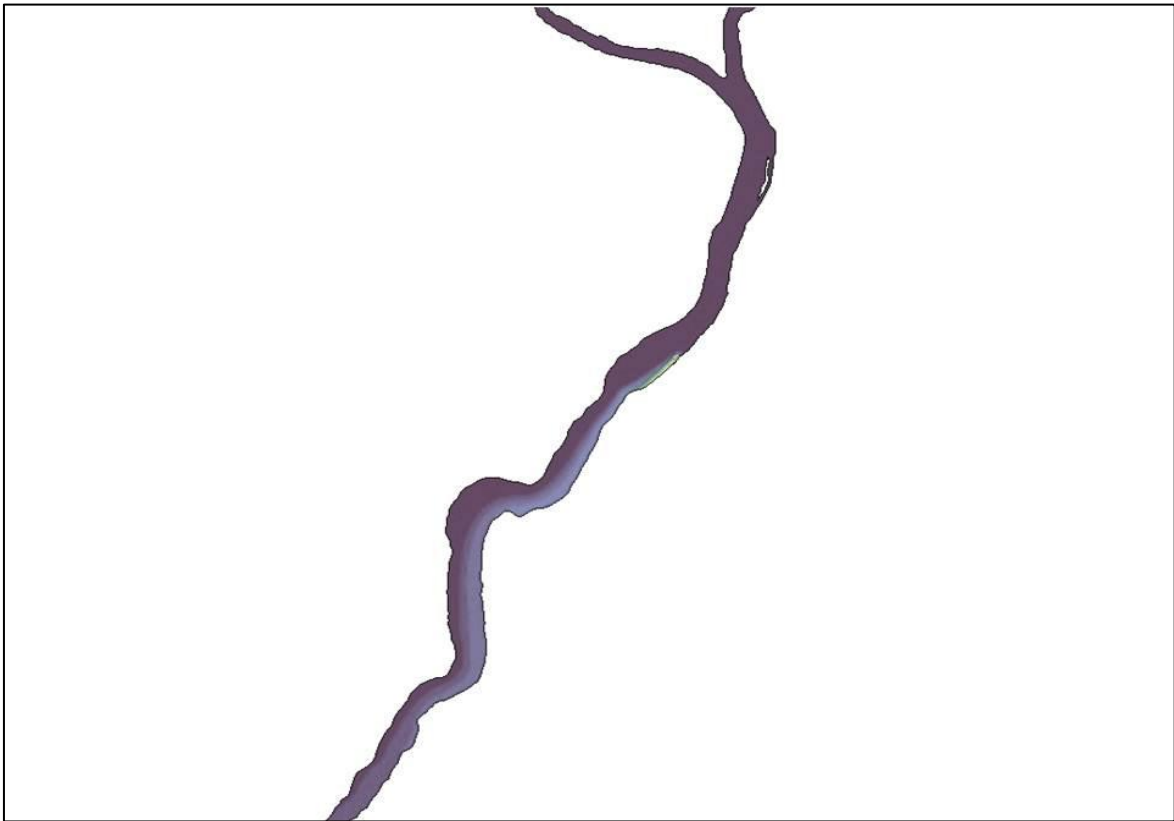


# CHALMERS



## Hydrodynamic and Microbial Modeling of a Drinking Water Source

*Master of Science Thesis in the Master's Programme Geo and Water Engineering*

AXEL EMANUELSSON  
JOHANNES SENNING

Department of Civil and Environmental Engineering  
*Division of Water Environment Technology*  
CHALMERS UNIVERSITY OF TECHNOLOGY  
Gothenburg, Sweden 2012  
Master's Thesis 2012:145



MASTER'S THESIS 2012:145

# Hydrodynamic and Microbial Modeling of a Drinking Water Source

*Master of Science Thesis in the Master's Programme Geo and Water Engineering*

AXEL EMANUELSSON

JOHANNES SENNING

Department of Civil and Environmental Engineering  
*Division of Water Environment Technology*  
CHALMERS UNIVERSITY OF TECHNOLOGY  
Gothenburg, Sweden 2012

Hydrodynamic and Microbial Modeling of a Drinking Water Source

*Master of Science Thesis in the Master's Programme Geo and Water Engineering*

AXEL EMANUELSSON

JOHANNES SENNING

© AXEL EMANUELSSON & JOHANNES SENNING, 2012

Examensarbete / Institutionen för bygg- och miljöteknik,  
Chalmers tekniska högskola 2012:145

Department of Civil and Environmental Engineering

Division of Water Environment Technology

Chalmers University of Technology

SE-412 96 Gothenburg

Sweden

Telephone: + 46 (0)31-772 1000

Cover:

The cover illustrates a modelled release of contaminated water into the river Glomma.

Chalmers Reproservice / Department of Civil and Environmental Engineering  
Gothenburg, Sweden 2012

*Hydrodynamic and Microbial Modeling of a Drinking Water Source*

*Master of Science Thesis in the Master's Programme Geo and Water Engineering*

AXEL EMANUELSSON

JOHANNES SENNING

Department of Civil and Environmental Engineering

Division of Water Environment Technology

Chalmers University of Technology

ABSTRACT

Pathogen contamination of drinking water sources implicates risks for outbreaks of waterborne diseases and is a major health issue throughout the world. Within the European Union, viruses and other pathogens originating from fecal contamination are considered to be the prime concern related to drinking water. In order to predict the presence of pathogens and manage the risk of outbreaks it is essential to understand the transport and fate processes of microbes in drinking water sources.

In this study, which is a part of an EU-project, a coupled hydrodynamic-microbiological modeling approach has been used to forecast microbial concentrations in a drinking water source. The study object was the river Glomma in Norway, and the hydrodynamics of the river were simulated using a three-dimensional model MIKE 3 FM (Flexible mesh). Validation of the modeled hydrodynamics was performed by comparing the modeling results with measured values of water level and water velocity at different locations in the river. The validation confirmed that the model represents the river hydrodynamics well.

Based on the output from the hydrodynamic model, transport of norovirus and *E.coli* in the river was simulated using ECO Lab module. A hypothetical scenario was analyzed with the coupled model where a wastewater treatment plant located upstream the raw water intake releases untreated wastewater due to reconstruction. The results showed significantly increased microbial concentrations with *E.coli* concentrations exceeding 500 *E.coli*/100ml, which is above the guidelines for safe raw water.

The obtained results demonstrated that coupled hydrodynamic-microbiological modeling is a useful approach for simulating microbial spread in drinking water sources. Furthermore, the approach is useful for analyzing specific future scenarios.

Key words: Hydrodynamic modeling, drinking water, waterborne pathogens norovirus, *E.coli*, MIKE 3, ECOLab

*Hydrodynamisk och mikrobiologisk modellering av en ytvattentäkt*  
*Examensarbete inom civilingenjörsprogrammet Geo and Water Engineering*

AXEL EMANUELSSON

JOHANNES SENNING

Institutionen för bygg- och miljöteknik

Avdelningen Vatten Miljö Teknik

Chalmers tekniska högskola

## SAMMANFATTNING

Mikrobiella föroreningar av dricksvattentäkter utgör en risk för utbrott av vattenburna sjukdomar och är ett stort hälsoproblem i hela världen. Inom EU anses det främsta hotet mot dricksvattenkvaliteten vara virus och andra patogener som härrör från fekal förorening. För att kunna förutsäga förekomsten av patogener i dricksvattentäkter och hantera risken för utbrott är det betydelsefullt att förstå transportprocesserna.

I denna studie har en kopplad hydrodynamisk och mikrobiologisk modell använts för att simulera patogentransport och koncentrationer i en dricksvattentäkt. Studien är en del av ett EU-projekt och simuleringen genomfördes på älven Glomma i Norge. Programvaran MIKE 3 FM (Flexible Mesh) användes för att beskriva hydrodynamiken och vattentransporten i tre dimensioner. Validering av den simulerade hydrodynamiken utfördes genom att jämföra modellerade värden med uppmätta värden på vattennivåer och flödes hastigheter vid olika mätpunkter utmed älven. Från valideringen av älven konstaterades att resultatet från simuleringarna representerar älvens hydrodynamik på ett tillfredsställande sätt.

Baserat på den hydrodynamiska modellen simulerades ett scenario där ett reningsverk uppströms råvattenintaget var tvunget att brädda allt vatten orenat ut i recipienten på grund av ombyggnation. Resultaten visade på kraftigt förhöjda mikrobiella koncentrationer vid dricksvattenintaget med koncentrationer av *E.coli* överskridande Svenskt Vattens riktvärde på 500 *E.coli*/100ml.

Strategin att använda sig av en kopplad hydrodynamisk och mikrobiologisk modell bedöms vara väl lämpad för att förutspå patogenkoncentrationer i dricksvattentäkter. Vidare kan metoden även vara användbar för att analysera och utvärdera olika framtidsscenario.

Nyckelord: Hydrodynamisk modellering, dricksvatten, vattenburna patogener, norovirus, *E.coli*, MIKE 3, ECOLab

# Table of Contents

ABSTRACT	I
SAMMANFATTNING	II
TABLE OF CONTENTS	III
PREFACE	IV
1 INTRODUCTION	1
1.1 Aim and objectives	1
2 BACKGROUND	2
2.1 Problem description	2
2.2 Pathogens and fecal indicators in drinking water	3
2.3 The VISK Project	4
2.4 Theoretical background	5
3 MATERIALS AND METHODS	6
3.1 Study area	6
3.2 Model Setup	10
3.2.1 Input data and validation data	12
3.2.2 Domain specification	14
3.2.3 Mesh Generation	16
3.2.4 Simulation of hydrodynamics	19
3.2.5 Model setup and simulation of microbial dynamics (ECO Lab)	23
4 RESULTS	26
4.1 Mesh validation results	26
4.2 Sensitivity of parameter values	27
4.3 Hydrodynamic validation results	30
4.4 Output from simulation of scenarios	35
5 ANALYSIS AND DISCUSSION	39
6 AREAS OF FURTHER INVESTIGATION	41
7 CONCLUSION	42
8 BIBLIOGRAPHY	43

## Preface

This master thesis has been performed, during the autumn of 2012, as the final project at the Department of Civil and Environmental Engineering at Chalmers University of Technology. The study has been executed to model the hydrodynamics of a water source as well as the microbial spreading of norovirus and *E. coli* within it. This project has been part of the VISK project, which is an EU project aiming at preventing virus spreading in drinking water.

First, we wish to thank our supervisors Ekaterina Sokolova and Thomas Pettersson for their interest and great input, help and criticism, which motivated us to work hard during long hours.

Many people have been contributing to our study in different ways. Much data have been gathered and used in various steps of the modeling process. Data have been received from Søren Kristensen at NVE and Jens Kristian Tingvold at GLB, both which must be seen as key persons regarding the acquisition of hydrodynamic data. Furthermore, Lena Solli Sal at NVE has provided essential data for the microbiological modeling.

We are also grateful to VISK Norwegian project leader Mette Myrmel and her Ph.D. student Ricardo Rosado that have been helpful even though we understand that you have been busy. Furthermore, giving us the invaluable opportunity to get out from our hot and oxygen poor office and come to Norway to see the actual river Glomma and perform important data acquisition.

Finally, an additional thank to Ekaterina who has been a great sounding board during the whole project and read our report and filled it with comments, all of great significance!

Gothenburg, June 2012

Axel Emanuelsson and Johannes Senning

# 1 Introduction

Drinking water contaminated with viruses and other pathogens is throughout the world a major health issue which every year claims millions of lives (Cloete, 2004). According to the World Health Organization, WHO, the presence of microbial pathogens caused by fecal contamination of drinking water sources, is considered the prime concern regarding drinking water within the European Union (WHO, 2012). This concern has in the recent years been emphasized in the Scandinavian countries by a number of outbreaks of gastrointestinal diseases. Gastrointestinal diseases are an important health concern and implicate major expenses to the society every year (Tran & Brytting, 2010).

Fecal contamination in raw water sources often originates from release of sewage water since many watercourses serve both as raw water sources and recipients of wastewater (Häfliger, Hübner, & Lüthy, 2000). Fecal contamination of drinking water sources is usually detected by measuring the concentrations of fecal indicators, from which the needs of water treatment and consumer risk is being assessed.

However, the presence of fecal indicators does not necessarily suppose that pathogens are present. Likewise, even though no fecal contamination can be established, pathogens may nevertheless be present which is a major drinking water concern (WHO, Guidelines for Drinking-water Quality, 2008). Previous research has therefore suggested that pathogen concentrations in raw water can be predicted using coupled hydrodynamic-microbiological computer models that describe the fate and transport of the pathogens in a drinking water source (Harwood, et al., 2005).

Models can be used for dimensioning drinking water treatment plants and to plan mitigation measures in terms of fecal contamination of drinking water sources. Furthermore, hydrodynamic-microbiological transport models can be used to provide data for microbial risk assessment, i.e. to estimate consumer health risks.

## 1.1 Aim and objectives

The purpose of this master's thesis is to describe the hydrodynamics and spread of microbial contamination in a raw water source, the river Glomma in Norway, using a coupled hydrodynamic and microbiological modeling approach. The model is a part of a project funded by the European Union where the outputs are to be connected to future risk assessments and QMRA (Quantitative Microbial Risk Assessment). Furthermore, the model should enable the possibility of investigating different hypothetical scenarios of microbial spread in the raw water source.

The more specific objectives are:

- to gather input and validation data for the model from project partners, national authorities and agencies, and where data is insufficient, to gather data in the field;
- to construct a computational mesh, which represents the bathymetry of the river Glomma;
- to simulate the hydrodynamics of the river Glomma and validate the output towards measured data;
- to model the spread of pathogens and indicator organisms within the river, both for the present situation and for hypothetical scenarios;

## 2 Background

This chapter includes a brief description of the problem regarding microbial contamination of drinking water. In this chapter the concern of waterborne virus outbreaks becoming more frequent in the future is introduced and different preventive measures in this context are discussed. Furthermore, the EU-project VISK that this thesis is a part of is presented, and a short theoretical background regarding the computational models used in this thesis is provided.

### 2.1 Problem description

Discharges from wastewater treatment plants (WWTP) into watercourses used as raw water sources constitute an important source of waterborne human pathogens (Kukkula & Arstila, 1997). Even though the density of pathogens is reduced by a factor of 10-1000 in the treatment processes before the water is released, the discharged wastewater in general contains human pathogens (Henze, 2002).

Moreover, when overflow occurs at WWTPs, untreated wastewater which contains pathogen concentrations magnitudes higher, is discharged into the raw water source. Overflow occurs when the water flow into the WWTP is higher than the capacity of the WWTP which may occur in e.g. periods with heavy precipitation or snow melt in the spring (Aasand, 2011). Furthermore, release of untreated wastewater may occur due to different kinds of operation stoppage during reconstruction of the WWTP or due to failures at the WWTP.

Furthermore, due to altered weather patterns the number of extreme rains is expected to rise (IPCC, 2007) which would cause more regular overflows at WWTPs (Niea, Lindholma, Lindholmb, & Syversen, 2009). In addition, the quantity of wastewater that needs to be treated is expected to increase due to projected increase in population in the Scandinavian countries (SCB, 2010). More frequent overflows at WWTPs and an increasing load of wastewater may aggravate the problem of contamination of drinking water sources with human pathogens.

It is possible to evaluate the health threat due to transport of pathogens in the rivers from a risk perspective. The health risk originating from fecal contamination of a raw water source is often described with a conceptual model which maps the hazards towards the drinking water consumers (Lindhe, 2008). Often there are many parameters that need to be taken into account and the most important ones can be described with the source-pathway-receptor concept (Sneddon et al 2009). The source-receptor-pathway concept is used to describe a watercourse being utilized both as a raw water source and as a recipient of wastewater (Figure 1).

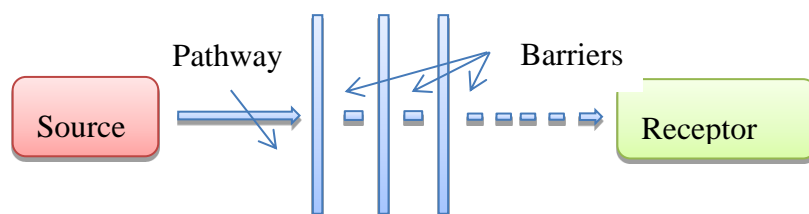


*Figure 1 Schematic representation of the system from a risk analysis perspective. The wastewater treatment plants are the sources, the river is the pathway, the drinking water treatment plant contains the barriers and the consumers are the receptors.*

- The wastewater treatment plants are the *sources* from which the pathogens are spread.
- The river is the *pathway* in which the transport of pathogens occurs.
- The drinking water treatment plant with its treatment steps constitutes the *barriers*.
- The drinking water consumers that are provided with water from the actual treatment plant are the *receptors*.

## 2.2 Pathogens and fecal indicators in drinking water

The most widespread health risk associated with drinking water is infectious waterborne diseases caused by pathogens such as viruses, bacteria and parasites (e.g. protozoa and helminths) (WHO, 2008). In order to manage the risk to provide safe drinking water, the treatment steps in water treatment plants are dimensioned in regard to the assessed abundance of pathogens in the raw water.

However, the pathogenic organisms themselves are often difficult and time consuming to detect (WHO, 2008). Since pathogens generally originate from fecal contamination, the presences of fecal indicators are analyzed instead of the actual pathogens. An indicator organism is not pathogenic itself but should be present whenever enteric pathogens are present. Furthermore, it should not grow in water by itself; the density of the indicator should have direct relationship to the density of the pathogen and it should be easy to detect.

Conversely, in the reality no indicators meet all the criteria and for many pathogens there are no indicator organisms to represent them in a good way and for many pathogens the correlation between pathogen density and indicator density is weak (Harwood, et al., 2005). Pathogens can in some cases be abundant even though no fecal contamination is detected, as in Östersund, Sweden, where an outbreak of the parasite *Cryptosporidium* made 20000 people ill in 2010 (SMI, 2011).

For many strains of infectious enteric viruses, the correlation with fecal indicators is weak and viruses might be present regardless the presence of indicators (Harwood, et al., 2005). Since viruses are smaller than bacteria and enteric parasites they are often difficult to reduce in drinking water treatment plants (WHO, 2008). Moreover, enteric viruses such as noroviruses can be pathogenic even in very low concentrations which make them important to consider in regard to safe drinking water (Häfliger, Hübner, & Lüthy, 2000). The abundance of virus in untreated wastewater varies prominently over the year (Hewitt, 2011).

Of the reported cases of waterborne disease outbreaks in Sweden, in a substantial part of the cases the outbreak could never be traced back to a certain contagium but much indicates that the source is viral (VISK, 2012).

The survival fate of pathogens within a water course can differ greatly and many parameters such as temperature, salinity, sun radiation etc. influence the inactivation time (Herzog, Bhaduri, Stedtfeld, Gregoire, & Farhan, 2010). Many of the most common waterborne pathogens (e.g. adenoviruses and noroviruses) have high persistence towards inactivation but cannot multiply outside their host (WHO, 2008).

## 2.3 The VISK Project

In order to manage the predicted increase of pathogens in raw water, an EU project VISK (Virus i Vatten Skandinavisk Kunskapsdatabas) with the overall purpose of reducing the societies vulnerability to waterborne virus outbreaks was initiated. The aim of the project is to gather information and knowledge to be able to maintain today's high quality of drinking water in Scandinavia, despite the predicted changes in climate and population size.

The project is a part in the InterReg initiative, which is a line of cooperation programs funded by the European Regional Development Fund with the purpose of increasing the cooperation across the nation borders within the European Union. It is an approach to diminish the nation borders and instead work on regional basis, since problems such as environmental issues are sometimes more similar within a multinational geographic region rather than in a specific country. The VISK-project applies to the InterReg region Öresund-Kattegat-Skagerrak which is located in Sweden, Norway and Denmark around the strait Öresund-Kattegat-Skagerrak that connects the North Sea and the Baltic Sea (Figure 2).



Figure 2 Map of the areas within Norway, Sweden and Denmark that are included within the InterReg region Öresund-Kattegat-Skagerrak (InterReg, 2012).

The VISK project is focused on large rivers as raw water sources and the rivers Glomma and Göta Älv have been chosen to be studied in Norway and Sweden respectively. The large rivers are interesting because of their capacity of providing large quantities of raw water. In the river Glomma, for example, the current withdrawal of water is roughly only about 1/1000 of the average river flow, signifying that the potential of satisfying higher future demands of water is immense. However, the rivers are often used for many purposes and activities which may threaten the quality of the water.

This master's thesis is a part of the VISK-project with the purpose of mapping the virus spreading by computational modeling the hydrodynamics and microbiology of the river Glomma.

## 2.4 Theoretical background

All types of computational fluid dynamics (CFD) software are based on equations derived from fundamental laws of physics (Versteeg & Malalasekera, 2007). Navier-Stokes (NS) equations which constitute the backbone of most CFD software are based on the laws of continuity and are applications of concept of finite volumes (Andersson, 2009). The NS equations are non-linear partial differential equations which have to be solved numerically.

Since the turbulence in a fluid is difficult to model and demands immense computer power, for most engineering practices the NS equations are averaged with the Reynolds approximation, which means that the turbulence is averaged over a volume (Andersson, 2009). This approximation dramatically reduces the computational time.

The modeling approach used in this thesis is based on the three dimensional numerical solution of Reynolds averaged Navier-Stokes equations (DHI, 2011). Furthermore, Boussinesq approximation is being made and hydrostatic pressure is assumed (DHI, 2011). The laws of continuity (1) and momentum conservation (2) and (3) are central and are presented below. The equations of momentum conservation (2) (3) apply to x and y directions respectively.

$$\frac{\partial u}{\partial x} + \frac{\partial v}{\partial y} + \frac{\partial w}{\partial z} = S \quad (1)$$

$$\begin{aligned} \frac{\partial u}{\partial t} + \frac{\partial u^2}{\partial x} + \frac{\partial vu}{\partial y} + \frac{\partial wu}{\partial z} = f v - g \frac{\partial \eta}{\partial x} - \frac{1}{\rho_0} \frac{\partial p_a}{\partial x} - \frac{g}{\rho_0} \int_z^\eta \frac{\partial \rho}{\partial x} dz - \frac{1}{\rho_0 h} \left( \frac{\partial s_{xx}}{\partial x} + \frac{\partial s_{xy}}{\partial x} \right) \\ + F_u + \frac{\partial}{\partial z} \left( v_t \frac{\partial u}{\partial z} \right) + u_s S \end{aligned} \quad (2)$$

$$\begin{aligned} \frac{\partial v}{\partial t} + \frac{\partial v^2}{\partial x} + \frac{\partial uv}{\partial y} + \frac{\partial wv}{\partial z} = f u - g \frac{\partial \eta}{\partial y} - \frac{1}{\rho_0} \frac{\partial p_a}{\partial y} - \frac{g}{\rho_0} \int_z^\eta \frac{\partial \rho}{\partial y} dz - \frac{1}{\rho_0 h} \left( \frac{\partial s_{yx}}{\partial x} + \frac{\partial s_{yy}}{\partial y} \right) \\ + F_v + \frac{\partial}{\partial z} \left( v_t \frac{\partial v}{\partial z} \right) + v_s S \end{aligned} \quad (3)$$

$(x, y, z)$  are the Cartesian coordinates and  $(u, v, w)$  their corresponding velocity components;  $f$  is the Coriolis parameter;  $\eta$  is water level and  $h$  is the total water depth;  $\rho$  and  $\rho_0$  is water density and reference water density; and  $u_s$  and  $v_s$  are the resulting water velocities;  $v_t$  is the vertical turbulent viscosity;  $S$  is the point source related magnitude of velocity and  $g$  is the gravity acceleration;  $s_{xx}$ ,  $s_{xy}$ ,  $s_{yx}$  and  $s_{yy}$  are stress tensor components.

For the boundary conditions that are specified in the model, a Riemann solver is used to solve the governing equations numerically. For every time step the equations are solved numerically for each cell until the difference in the equations fall below a specified threshold.

In order to obtain stability in the model and to meet the Courant-Friedrichs-Lewy-condition (CFL-condition) high resolution of the computational grid requires a small time step (Courant, Friedrichs, & and Lewy, 1967). The condition claims that the time step must be kept small enough so that the water flow cannot flow through a whole cell in one time step (Courant, Friedrichs, & and Lewy, 1967).

### 3 Materials and methods

This chapter provides a description of the catchment area of the river Glomma and the specific stretch that is studied. It also describes the approach used to represent the hydrodynamics of a river in a computational model.

Furthermore, the main steps of the modeling process, such as construction of computational mesh, representation of the hydrodynamic features and input of microbiological aspects, are described.

#### 3.1 Study area

The river Glomma is 600 km, which makes it the longest river in Norway. The river Glomma originates in the highlands about 950 m above sea level in a glacial mountain area with peaks over 2000 m elevation. The river discharges in the southern part of Norway in the city Fredrikstad into the Oslo fjord, which is a part of the stait of Skagerrak. The catchment area of the river is populated by 600 000 people (L'Abée-Lund, et al., 2009) and covers 42 000 km<sup>2</sup> which is 11 % of the total area of the country (Figure 3).



Figure 3 Map of Norway shows the position of the catchment area of the river Glomma within the nation border (GLB, (Glommens och Laagens Brukserierforening), 2011) (Modified).

The water flow of the river Glomma varies strongly during the year. The yearly average discharge is 700 m<sup>3</sup>/s and the highest water flows occur during May-June when the snow melts in the northern part of the catchment area. In 1995 a flood

occurred when water flows up to 3 500 m<sup>3</sup>/s were registered; the flood had an estimated return time of 200 years (Figure 4) (NINA, ENRI (Norwegian Institute for Nature Research and Eastern Norway Research Institute), 2000).

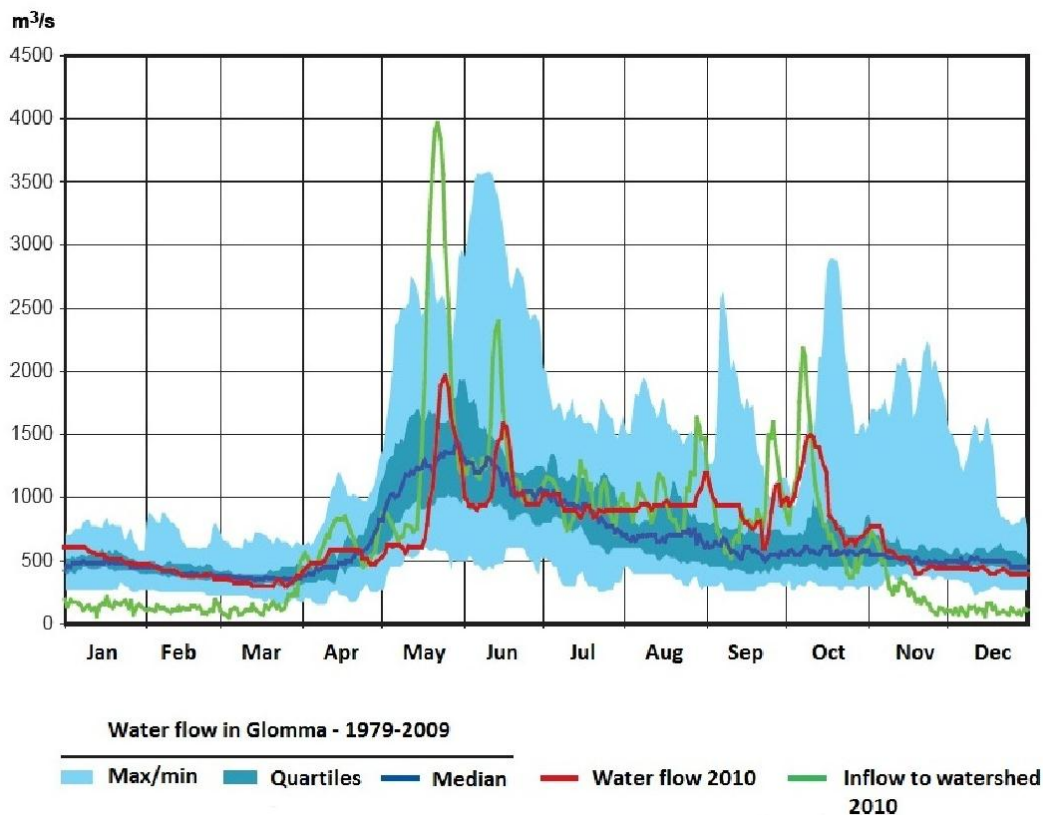


Figure 4 Water flow in the river Glomma. There are clear tendencies in the graph with two peak periods in the spring and autumn with lower flows in-between (GLB, (Glommens och Laagens Brukserierforening), 2011).

To be able to control the flow within the river Glomma natural reservoirs are used to increase the rivers storing capacity. One of many lakes that are used for this purpose is Lake Mjøsa, which the river Glomma flows through. It is Norway's largest lake and has a reservoir capacity of  $1312 \cdot 10^6 \text{ m}^3$ . The reservoir lakes are emptied during early spring to be able to store water during the spring flood, working as a buffer. This regulates the effect of the snow melting on the river flow and evens out the fluctuations over the year (GLB, (Glommens och Laagens Brukserierforening), 2011).

Due to its size, accessibility and high water quality (NRV & NRA, 2012) the river Glomma is used as a raw water source for 230 000 people. Out of the total number, 140 000 of the consumers are connected to the drinking water treatment plant Nedre Romerike Vannverk (Figure 5) (L'Abée-Lund, et al., 2009). Except being used as a drinking water source, the river is used as a recipient of wastewater, for hydropower, transportation, industrial and agricultural use as well as for recreational activities.

## The modeled stretch

The modeled stretch is approximately 40 km and extends from the fork where the river Vorma connects to Glomma north of the city of Årnes, to the city of Fetsund adjacent to where Glomma discharges into Lake Øyeren (Figure 5). It is surrounded by agricultural lowlands and hilly forested areas. There are numerous minor tributaries along the stretch, but only one, Ua, with a yearly mean flow exceeding 1 % of the river Glomma (NVE (Norwegian Water Resources and Energy Directorate), 2012).

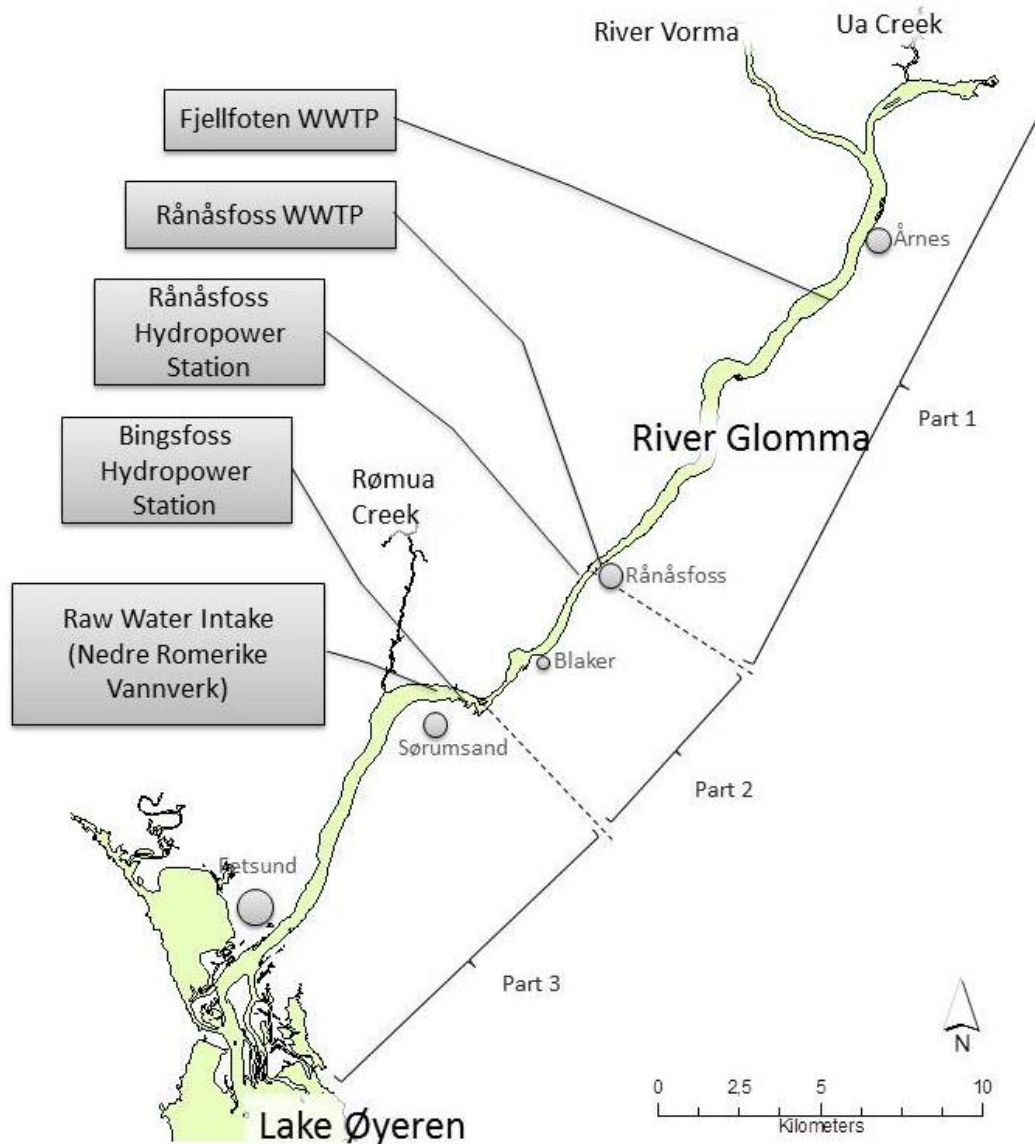


Figure 5 Map of the modeled stretch

The depth of the river is in the range 0 – 20 m, the mean depth is approximately 6 m (NVE (Norwegian Water Resources and Energy Directorate), 2012). The vertical drop of the stretch is approximately 20 m. Two hydropower stations along the stretch make up for most of the height drop. Hence, the vertical drop of the water surface and bottom slope before, in-between and after the two hydropower plants is rather small and the flow is subcritical. Since the flow is subcritical, it is mainly governed by the conditions downstream (Häggström, 2009) such as the water level in Lake Øyeren.

## **Hydropower stations**

The hydropower station in Rånåsfoss is the largest and reaches over the whole width of the river, while the one in Bingsfoss only covers half of the river. The hydropower stations are run-of-the-river plants, and have no storing capacity of water (Gundersen, 2012). For water flows in the river Glomma below the maximum capacity of the hydropower plants, the full flow is lead through the turbines. At flows above the maximum capacity of the hydropower plants, water is released besides the turbines. The turbine capacity is 940 m<sup>3</sup>/s at Rånåsfoss and 820 m<sup>3</sup>/s at Bingsfoss hydropower plants (Akershus Energi AS, 2012).

## **Wastewater treatment plants**

Along the modeled stretch there are two wastewater treatment plants that use the river as recipient for treated water. The largest WWTP, Fjellfoten, is located south of the city Årnes and has approximately 14500 PE connected and processes on average 2800 m<sup>3</sup>/day (Viak Asplan, 2012). Another WWTP is located in the city Rånåsfoss and has a capacity of 800 PE and processes on average 200 m<sup>3</sup>/day (Asplan Viak, 2012). Overflows occur and in Rånåsfoss this has happened 17 times during 2011 (Sinkerud, 2012). The larger WWTP is subject to reconstruction 2012 and will release all water untreated for 6 months starting from May 2012 (Håkonsen, 2012).

## **Drinking water treatment plant**

The drinking water treatment plant Nedre Romerike Vannverk (NRV) has its intake for raw water located close to the city of Sørumsand (Figure 5). The intake is placed in the river Glomma 2 meter above the river bed and 10 meter below the average surface level. The intake was previously located at the mouth of the tributary creek Rømua, 2 km downstream from the present location, but was moved due to large variations in the water quality caused by Rømua. From the raw water intake, the water is pumped to 120 meters height above Glomma from where it flows by gravity to the drinking water treatment plant (NRV & NRA, 2012).

NRV are providing 143 000 consumers with drinking water and produces an average of 42 000 m<sup>3</sup> per day with a total capacity of 100 000 m<sup>3</sup> per day (Solli Sal, 2012). The daily volume produced fluctuates over the year and can increase by 50 % during dry summer periods. The production lines within the treatment plant are separated and can produce water independent of one another. This safety precaution ensures that water can be delivered to the customers even if one line breaks or has to be shut down because of maintenance reasons (NRV & NRA, 2012).

NRV is equipped with chemical precipitation, sedimentation, filtration and disinfection processes. Furthermore, an UV treatment step is being implemented in 2012, as an additional barrier (NRV & NRA, 2012).

## 3.2 Model Setup

The hydrodynamic conditions in the river Glomma were modeled using the simulation software MIKE 3 FM (Flexible Mesh) developed by DHI (DHI, 2011). The model is based on the numerical solution of the three dimensional incompressible Reynolds averaged Navier-Stokes equations.

For many applications when modeling rivers, modeling in two dimensions may be enough, assuming the water speed to be undiversified in the vertical dimension. However, in this project a three dimensional model has been used to be able to describe the spread of contamination in three dimensions.

The hydrodynamic module is developed for subcritical flowing conditions; hence, situations where supercritical flow occurs must be treated with care (DHI, 2011).

The hydrodynamic and microbiological modeling of the river Glomma has been carried out according to the different steps presented in the conceptual model (Figure 6) presented on the next page.

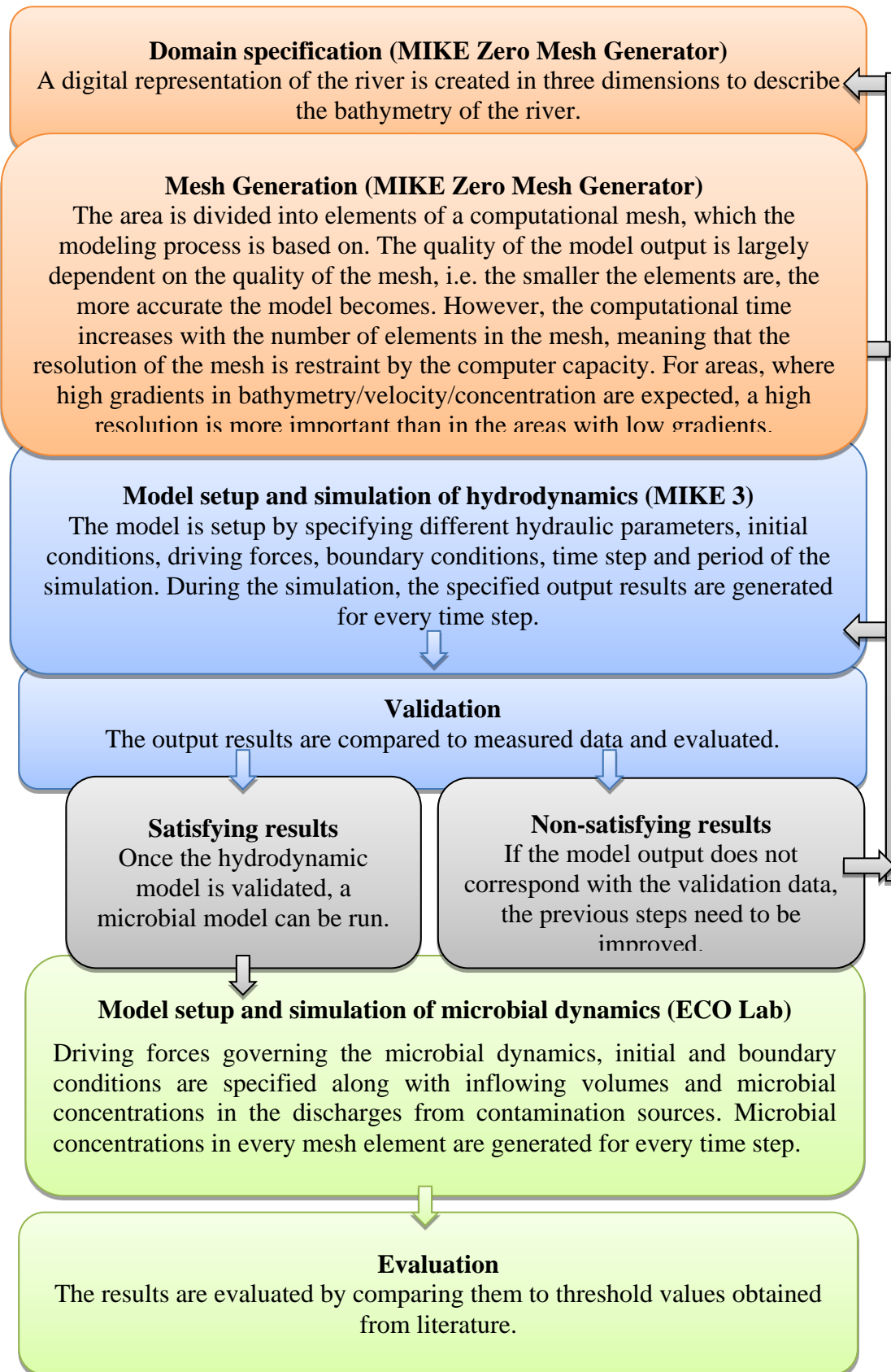


Figure 6 Flow chart of the conceptual model governing the modeling process. The arrows show how the different steps are connected to one another and that it is an iterative process.

### 3.2.1 Input data and validation data

Data have been obtained from partners within the VISK-project, national authorities and by measurements during a field survey. The data used for model construction and validation are described in Figure 7 and Table 1. The table is structured into three different categories depending on in which part of the modeling process the data have been used. The categories are *Mesh generation data*, *Hydrodynamic data* and *Microbiological data*.

All data time series cover the modeled time period of 2011-09-01 to 2011-09-31. This period was chosen since data was abundant for this period.

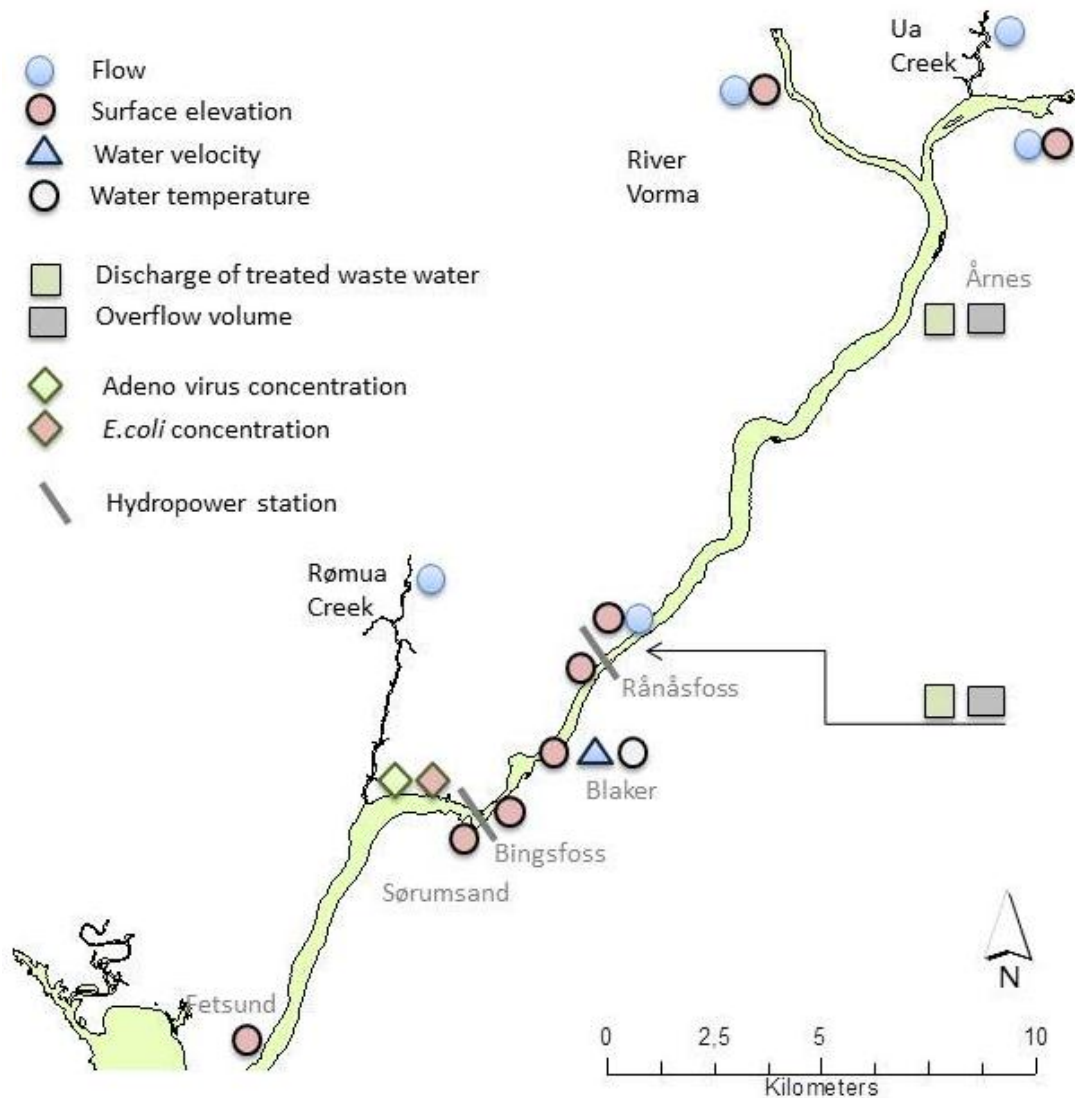


Figure 7 Map describing the location of the data. The legend gives information on the type of data used.

Table 1 the input and validation data for the modeling process. Data used as input are marked (i) and data used for validation are marked (v).

<b>Mesh generation data</b>	<b>Resolution</b>		<b>Source</b>
<b>Bathymetry</b>	1 m equidistance	(i)	NVE <sup>a</sup>
Bathymetry obtained in field survey	Cross sections every 200 m	(i)	Field survey led by NIVA <sup>b</sup>
River shoreline	1:50 000	(i)	NVE <sup>a</sup>
<b>Hydrodynamic data</b>	<b>Resolution</b>		<b>Source</b>
Water flow	24h	(i,v)	NVE <sup>a</sup> and GLB <sup>c</sup>
Water level	24h	(i,v)	NVE <sup>a</sup> and GLB <sup>c</sup>
Water velocity	24h	(v)	NVE <sup>a</sup> and GLB <sup>c</sup>
Water temperature	24h	(i)	NVE <sup>a</sup>
Wind speed and direction	6h	(i)	MET <sup>d</sup>
Inflow tributaries	24h	(i)	GLB <sup>c</sup>
<b>Microbiological data</b>	<b>Resolution</b>		<b>Source</b>
Conc. <i>E.coli</i> treated water at WWTP	Constant	(i)	(Henze, 2002)
Conc. <i>E.coli</i> untreated water at WWTP	Constant	(i)	(Henze, 2002)
Conc. Norovirus untreated at WWTP	Constant	(i)	(Hewitt, 2011), (Håkonsen, 2012)
Average discharge at WWTP (Fjellfoten)	Yearly average	(i)	NRA <sup>e</sup>

<sup>a</sup> Norwegian Water Resources and Energy Directorate  
<sup>b</sup> The Norwegian Institute for Water Research  
<sup>c</sup> Glommens og Laagens Brukseierforening  
<sup>d</sup> The Norwegian Meteorological Institute  
<sup>e</sup> Nedre Romerike WWTP IKS

### 3.2.2 Domain specification

The input data for drawing the geometry of the river were obtained from Norges Vass- og Energidirektorat (NVE). The data were obtained as raster files and depth curve shape files with the resolution of 1 m equidistance.

However, the extent of the depth data did not cover the entire stretch of the river. In part 2 (Figure 8), between the hydropower plants in Rånåsfoss and Bingsfoss, only a few cross sections existed which were regarded as not sufficient (Figure 8).

The modeled stretch was divided into three separate parts. Part 1: Fetsund/Ertesekken to Rånåsfoss, part 2: Rånåsfoss to Bingsfoss and part 3: Bingsfoss to Fetsund. The three parts are separated from one another by the hydropower plants (Figure 7) and (Figure 8).

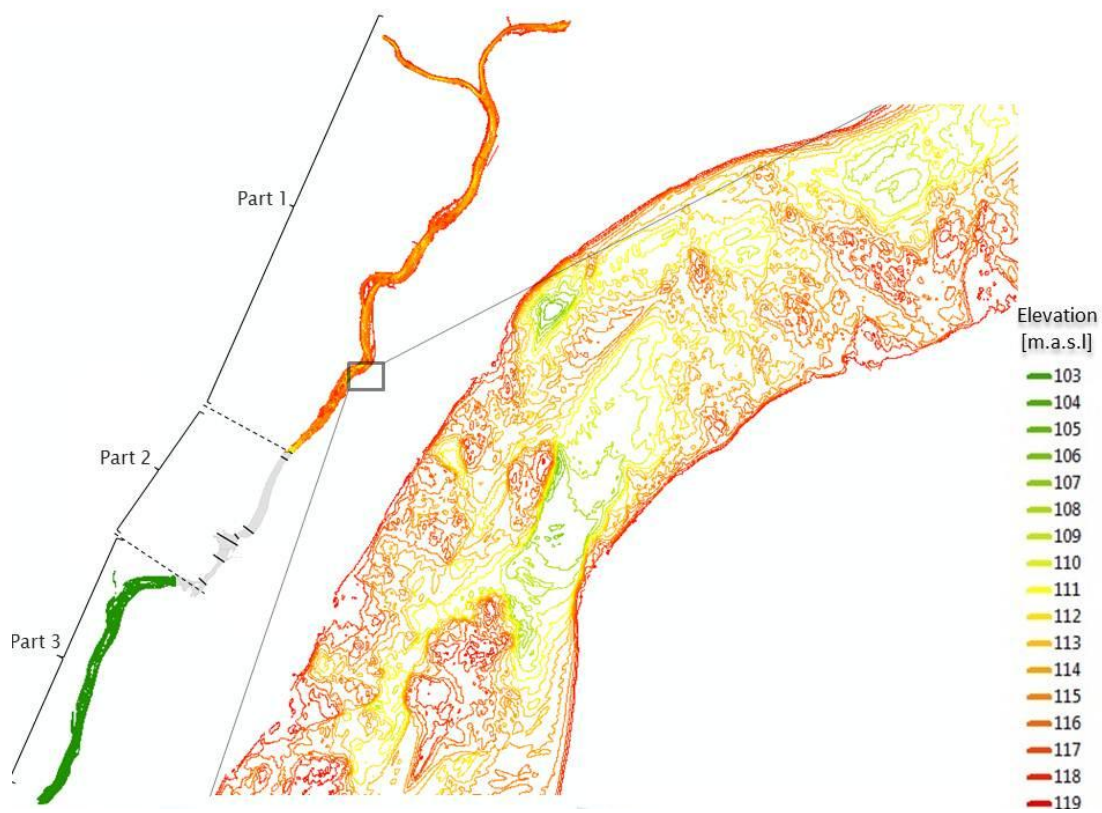


Figure 8 Map showing the existent data obtained from the beginning of the modeling process. The black lines on part 2 show where depth data along cross sections were obtained.

### Data acquisition by field measurements

In order to fill the gap of depth data in part 2, a field survey was carried out in the beginning of May 2012 in cooperation with the Norwegian Institute for Water Research (NIVA). The measurements were made in the river Glomma between Rånåsfoss and Bingsfoss with a single beam echo sounder mounted on a small boat (Figure 9). The echo sounder was connected to a GPS and a field computer that logged the depth and coordinates every second. From the measured depth values in part 2, an interpolation was performed to cover the remaining bathymetry area. Some of the data values provided by the echo sounder were sorted away due to unrealistic values, why the data in Figure 10 may appear discontinuous.



Figure 9 Left: The eco sounder connected to a field computer and a GPS. Right: Launching of the boat used for the field survey. In the background Rånåsfoss hydropower station is seen.

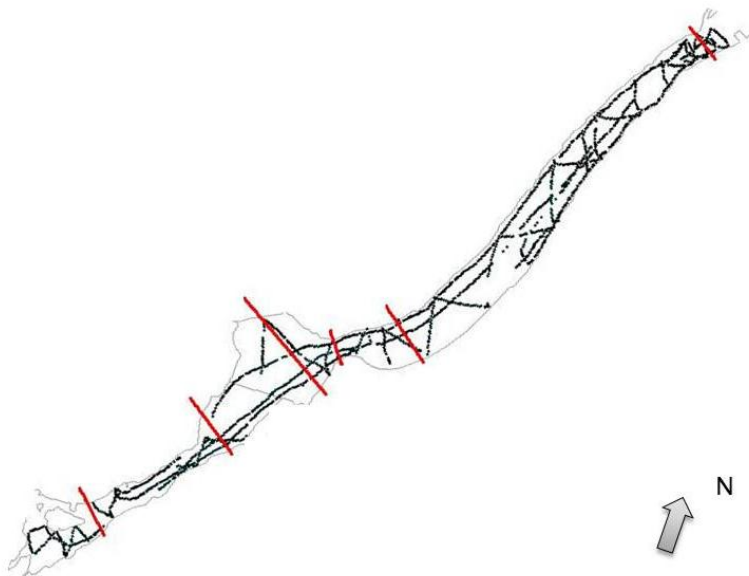


Figure 10 the pattern used in the field survey to map the bathymetry of the river on part 2. The red lines are depth cross-sections obtained from NVE.

### 3.2.3 Mesh Generation

Mesh generation was carried out using MIKE Zero Mesh Generator (DHI, 2011). A flexible mesh with triangular elements was used and the triangulation of the elements was executed with Delaunay triangulation (DHI, 2011). Three separate mesh files were constructed, one for each part.

The resolution of the mesh is a trade-off between quality and computational time and therefore careful effort was put into optimizing the mesh. The computational time step is restrained by the smallest mesh element and the number of computations is determined by the number of mesh elements (DHI, 2011). Sections of the river with varying hydrodynamics, such as a river bends or where the bathymetry changes, require higher mesh resolution. Hence, smaller mesh elements have been applied on such areas (Figure 11).

The minimum and maximum area and the number of elements in each part are presented in Table 2.

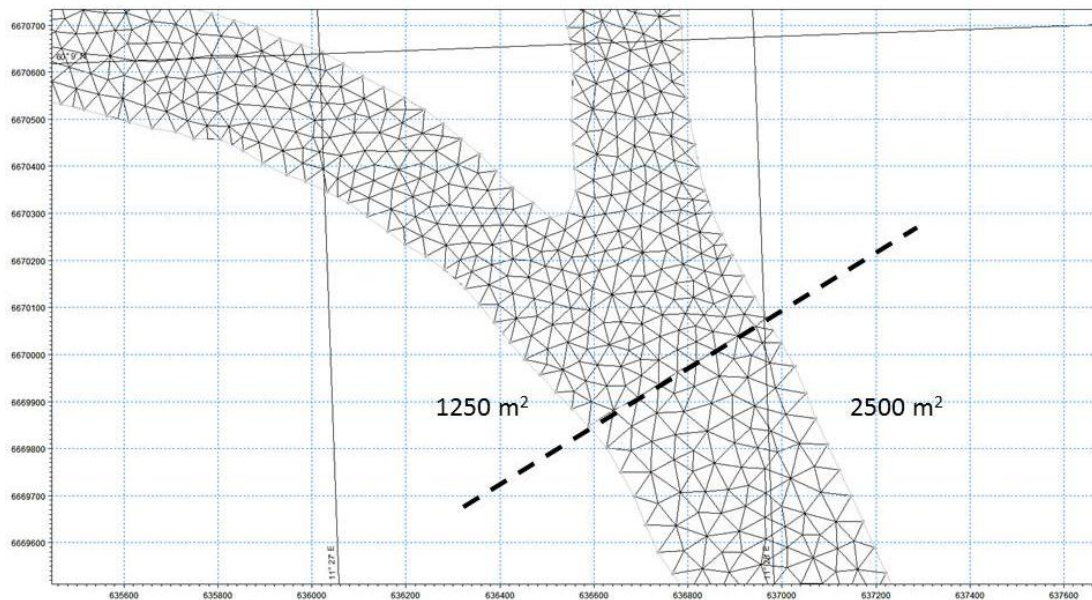


Figure 11 The area of the mesh element is set to maximum  $1250 \text{ m}^2$  in the river fork where the hydrodynamics are changing and to maximum  $2500 \text{ m}^2$  where the flow is more stable.

Table 2 characteristics of each part of the mesh.

Part	Smallest element area [ $\text{m}^2$ ]	Largest element area [ $\text{m}^2$ ]	Number of elements
1	323	2500	43005
2	314	1250	9745
3	361	2500	20030

At each mesh node a value of the bottom elevation was interpolated from bathymetry data with the natural neighbor method (DHI, 2011). After interpolating the depth, the mesh was further adjusted in order to obtain the same mean bathymetry values in cross sections of the mesh as in the bathymetry charts.

Since the sizes of the triangular elements are much greater than the resolution of the depth data, the interpolation often results in high difference in mean elevation between adjacent elements. This may result in incorrect simulation of the flow between the elements (Eriksson, 2012) and is common for the elements located close to the shoreline due to the high depth gradient. To avoid such complications, new values were assigned to the nodes of adjacent elements to decrease the difference in elevation between them.

In the vertical direction the river was divided into 5 sigma layers (DHI, 2011). The thickness of each layer is relative to the total depth and the proportions are displayed in Figure 12.

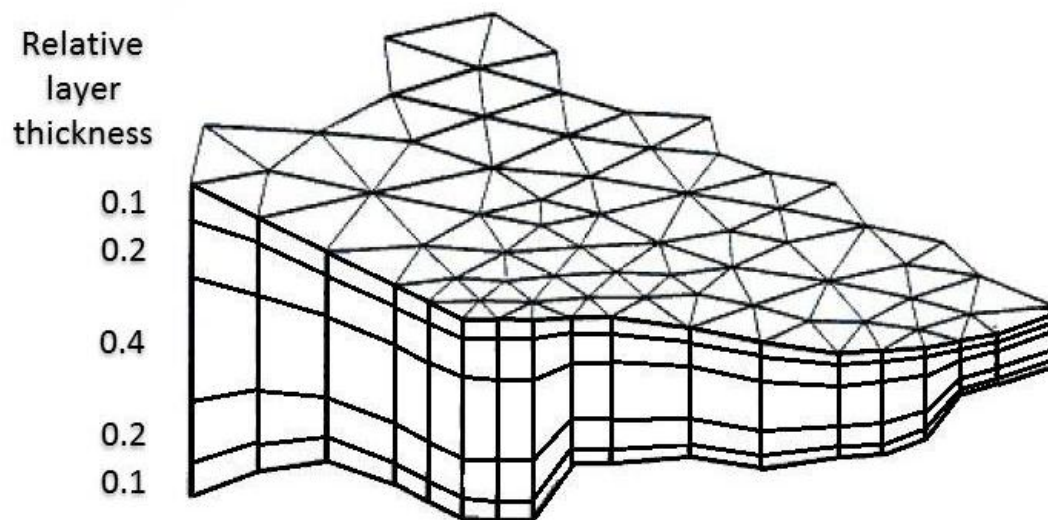


Figure 12 schematic figure displaying the relative thickness of the sigma layers (DHI, 2011)(Modified)

### Validation of the mesh

The bathymetry of the mesh was validated by comparing the average elevation in meters above sea level (m.a.s.l) with the riverbed's measured average elevation. The comparison was performed by dividing the river stretch into sections with uniform bathymetry (Figure 13). For each section, the average river bed elevation above sea level, was calculated and compared to the average elevation of the corresponding measured depth charts (Figure 14). The average elevation of each mesh section was acquired by averaging the mesh node values within the section. For the depth charts (obtained in raster format), the Spatial Analyst tool in the software ArcGIS was used to compute the mean value (Figure 14). The validation of the cross section of the river was done for 8 sections along the river stretch and subsequently, the mesh was modified until the difference in mean elevation between the mesh and depth charts was as low as possible.

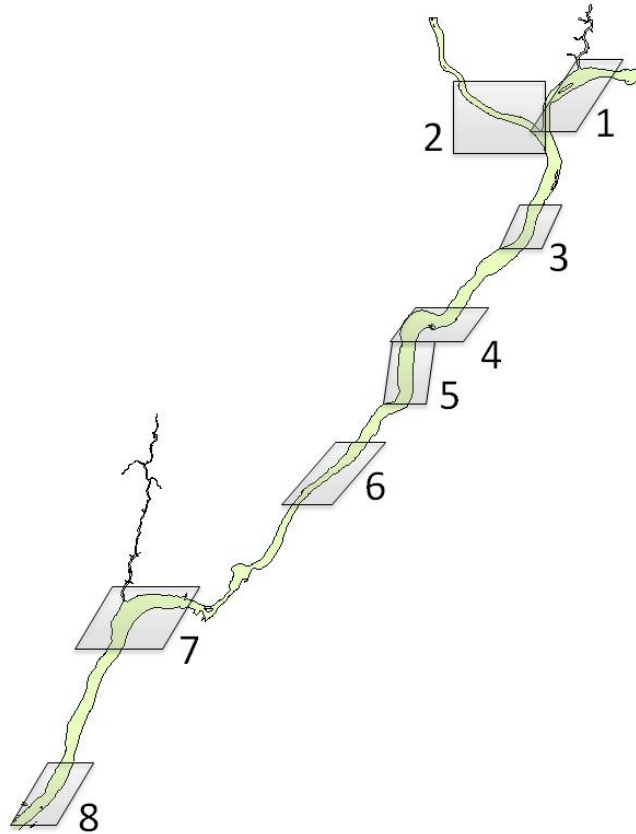


Figure 13 Location and extent of the different sections for which validation of the mesh was performed. The numbers marks the different sections.

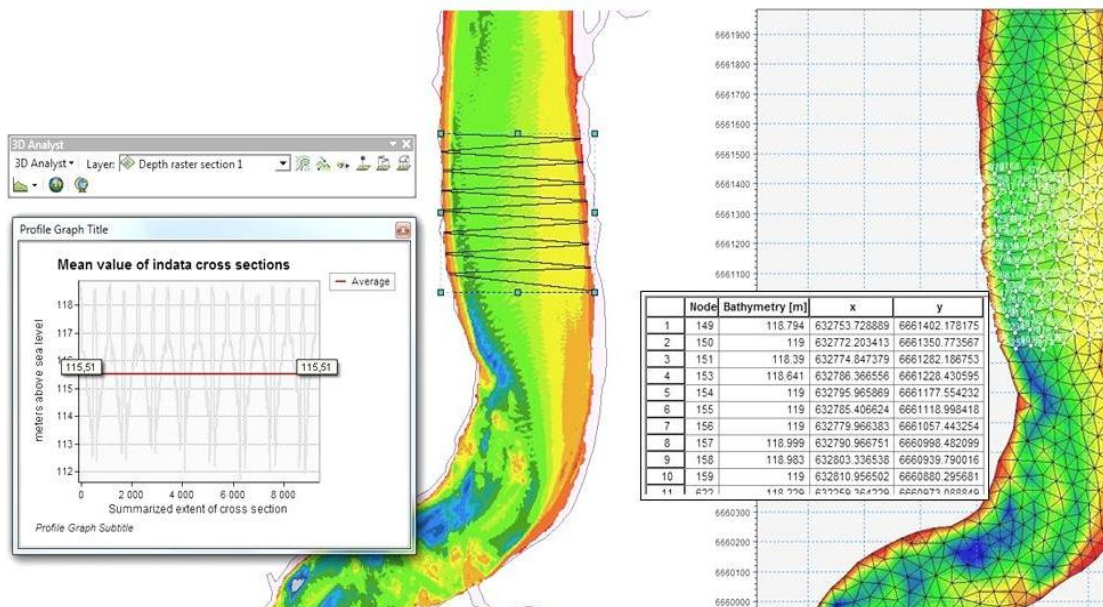


Figure 14 within a section, the average bathymetry values of the measured data (left) is compared to the average bathymetry value of the mesh.

Furthermore, comparisons of the geometry of cross sections were made. When designing the mesh, the intent was to keep the main features of the river section. An example is displayed in Figure 15.

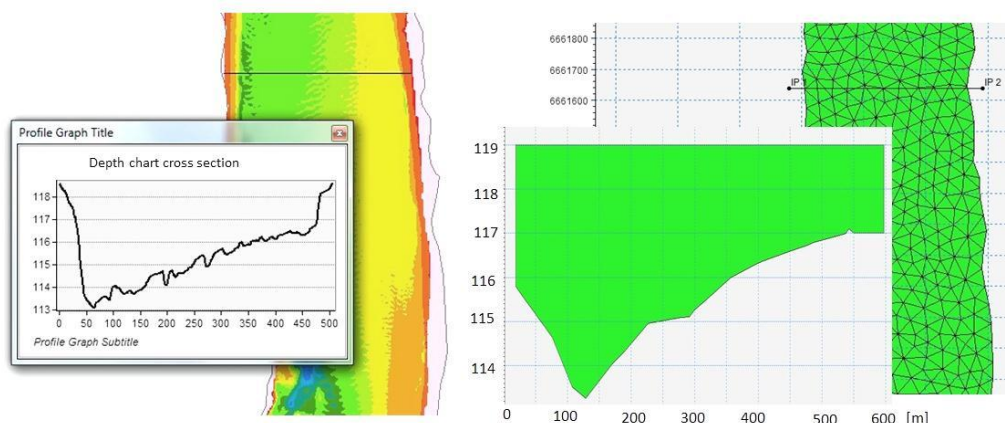


Figure 15 graphical image displaying the similarities between the measured cross section (left) towards the modeled cross section (right).

### 3.2.4 Simulation of hydrodynamics

Simulation of hydrodynamics was performed using MIKE 3 Flow Model Flexible Mesh (DHI, 2011). The time span for the simulation was 2011-09-01 to 2011-12-31 and output data were set to be generated every hour during the simulation period.

#### Boundary conditions

Input data for the boundary conditions were provided by NVE; this organization monitors the water flow and water level at different sites along Norwegian watercourses. The locations of the monitoring stations and the availability of data have been governing for the selection of model boundaries.

For the two northern boundaries of part 1 (Figure 5), time series of daily water flow over the cross section were used as boundary conditions. For the southern boundary of part 1, time series for the water level were used. Similarly, input data for part 2 and part 3 were also time series of water flow at the northern boundaries and water level at the southern.

#### Tributaries

Tributaries of the river Glomma were defined in the model as point sources using time series of water flow for each tributary. The two tributaries of most substantial size, Ua and Rømua, were included in the model (Figure 5). Water flow data for the tributaries were provided by NVE and GLB. Since the station measuring the flow in Rømua is located at a point where only half the tributary's catchment area provides water, the flow in Rømua was doubled as a rough estimation.

#### Hydropower stations

To handle the drop of height before and after the hydropower plants, the river was divided into three parts and hydrodynamics of each part were simulated independently of one another.

The hydropower station in Rånåsfoss, between part 1 and 2, consists of two turbine houses located on either side of the river (Figure 16, left). Since the both turbine houses on opposite sides of the river are run through by approximately the same water flow, it was assumed that any concentration gradient along the cross section will last through the power station. Therefore, the concentration gradient discharged out of part 1, was set to remain into part 2.

For the hydropower station in Bingsfoss, between part 2 and part 3, no gradient was set to last since the total water flow is discharged at one location (Figure 16, left). It is assumed that the discharged water is completely mixed due to turbulence. During high water flow in the river Glomma, water can also be released at an additional point (Figure 16, left, dashed arrow), which was not included in the model. It is assumed that during such occasions, the turbulence will be sufficient to eliminate the gradient in concentrations.

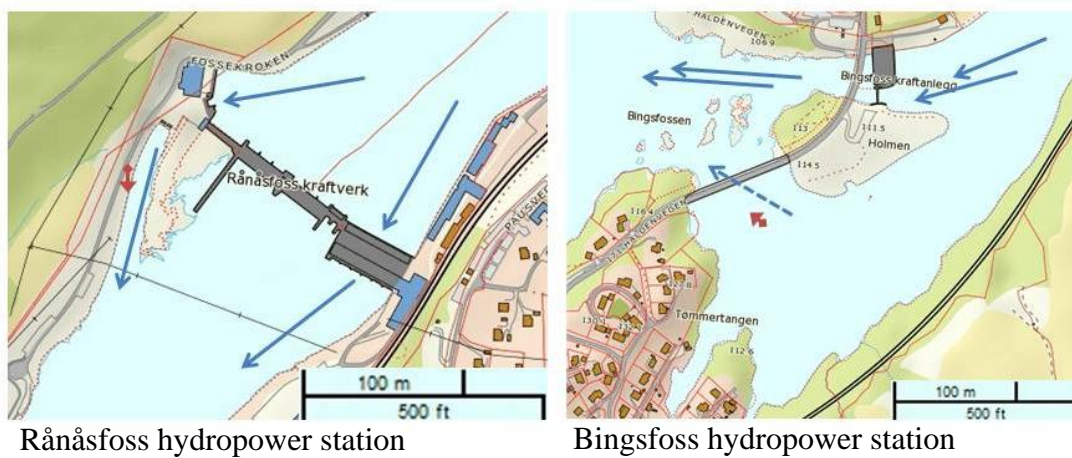


Figure 16 Distribution of water flow through the hydropower stations in Rånåsfoss (left) and Bingsfoss (right). The dashed arrow in the left picture shows where discharge occurs during high water flow. The red markers display from where the photos below were taken



Figure 17 Outlet from west turbine at Rånåsfoss hydropower station 2012-02-29



Figure 18 Crest near Bingsfoss hydropower station where water overflows during high water flow 2012-05-07

## **WWTP discharge and raw water intake**

The discharges from the two WWTPs were defined as sources with constant flow based on their yearly average treated water volume. The location of the sources was based on information from personnel involved with the operation at each WWTP. The drinking water intake was also modeled with a simple source but with a water flow out of the river.

## **Forcing data**

Wind speed and direction data were used as a forcing in the model. The wind forcing was defined by time series measured on a monitoring station 20 km north-west of Årnes.

## **Parameter values**

As was stated in the conceptual model (Figure 6), the modeling process has been carried out as a feedback loop, evaluating the results after each run to refine the model. The model was calibrated by adjusting the parameter values to obtain output results that match measured data.

A sensitivity analysis was made in regard to the bed roughness which was the parameter mainly used to calibrate the model. The analysis was done by running the same simulation with five different values for the bed roughness and was performed separately for each of the three parts. In a natural riverbed, the bed roughness is approximately 0.03-0.9 m (Chow, 1959). The bed roughness values 0.1, 0.3, 0.5, 0.7 and 1 m were tested and the resulting difference in water level recorded. The values of bed roughness that responded to water levels closest to the measured ones were used in the final hydrodynamic model. The full result of the sensitivity analysis is presented in the results chapter.

The simulated period over which the sensitivity analysis and the calibration were performed was chosen from the 2011-09-18 to 2011-10-31. The period was reduced compared to the hydrodynamic simulation period in order to validate the model for a different period than the period used for calibration. However, the calibration period was selected to include periods with both high flow and average flow. Regarding water levels, the locations that were used for the calibration were: a point close to the northern boundary for part 1; a point in the middle of the stretch close to Blaker for part 2; and a point just below the hydropower station for part 3 (Figure 5).

Furthermore, a coarser sensitivity analysis was also performed to assess the wind forcing influence on the water level and water velocity in different layers of the model. Two simulations were carried out for part 2 which were identical except that one simulation included wind forcing and the other did not. The chosen time period was 2011-10-08 (24h) and wind was abundant from north-east at 10 m/s. The direction of the river is approximately the same for part 2. To evaluate how the wind forcing affects the distribution of water flow over the cross section an arbitrary mesh element north of Blaker was regarded. Velocities in the top and bottom layer as well as the depth averaged velocity were recorded with and without wind. Moreover, the wind forcing's influence on the water level was reviewed.

Assigned parameter values used in the hydrodynamic simulation are specified in Table 3.

Table 3 Parameter values used in hydrodynamic simulation.

Parameter	Value	Motivation
Bed roughness	0.5	Selected after multiple simulations where different values were tested.
Solution technique	Low order	Faster algorithm that reduces the computation time. Finer mesh was prioritized.
Wind friction	Constant: 0.001255	Default
Flood and dry	Disabled	Recommended to not include when EcoLab is used (Eriksson, 2012)
Vertical eddy viscosity	Log law formulation	Default
Horizontal eddy viscosity	Smagorinsky formulation	Default
Density	Barotropic density	Density was not set to depend on salinity since the river water is fresh.

### Validation of the hydrodynamic modeling

Validation of the hydrodynamic model is of high importance since the subsequent microbiological modeling is based on the hydrodynamic model. The validation of the hydrodynamics was done by comparing the hydrodynamic output and the measured values. Primarily, measured water levels, velocities and water flows were used for validation. The validation period reached from 2011-09-01 to 2011-12-31 which means that the major part of the period is not covered by the period for the calibration. Water levels were compared in the two north boundaries of part 1, downstream Rånåsfoss, in Blaker and downstream Bingsfoss (Figure 5). Water velocities were compared in Blaker which was the only location where velocity data were abundant. Moreover, data used for the velocity validation was not used in the calibration of the model which increases the reliability of the validation.

In addition, aerial photos have been used to visually evaluate the laminar flow and stirring of the river.

Since no three dimensional validation data was available, no validation of the water velocity distribution over the cross section could be made. However, in natural water courses the velocity is generally distributed as in Figure 19, with lower velocities close to the river bed and shoreline, and higher velocities central in the cross section and closer to the surface (Häggsström, 2009).

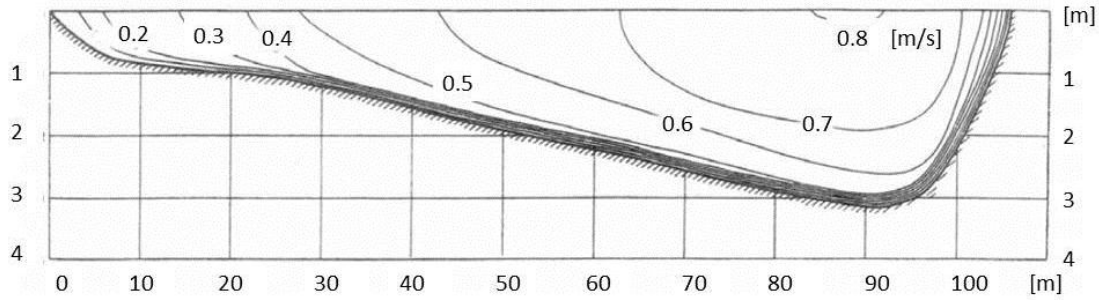


Figure 19 Measured velocities over a cross section in a natural course of a river (Hägström, 2009)

### 3.2.5 Model setup and simulation of microbial dynamics (ECO Lab)

Simulations of microbial transport were performed using MIKE 3 Flow Model Flexible Mesh connected to the EcoLab and Transport Module extensions (DHI, 2011). The microbial modeling was carried out for the bacterial fecal indicator *Escherichia coli* (*E. coli*) and for norovirus for different time periods and scenarios (Table 4). EcoLab was used to model transport and decay of *E. coli*. For simulating the transport of norovirus, the Transport Module was used and the decay was assumed to be 0 due to high persistence and short retention time in the river.

Table 4 The chosen simulation periods and the its coherent time step. When using small time steps shorter periods have to be chosen due to the time aspect. Therefore short time step was chosen when modeling the transport and spreading of a pulse release and a larger for the continuous overflow.

Scenario	Simulated period	Computational time step
Scenario 1	1 <sup>st</sup> of October -30 <sup>th</sup> of november	10 min (1 second tested)
Scenario 2	27 <sup>th</sup> – 29 <sup>th</sup> of November	1 sec

#### Microbiological model setup

The two most essential equations for the microbial simulations are the ones describing the inactivation and decay of the microorganisms (DHI, 2011) and are included in EcoLab. Equation (4) describes the change of *E. coli* concentration due to inactivation.

$$\frac{dC_f}{dt} = -k * C_f \quad (4)$$

Where  $k$  is the decay coefficient for the *E. coli* and  $C_f$  is the concentration of *E. coli*.

Equation 5 describes the contributions to the decay coefficient due to salinity, solar radiation and temperature (Mancini, 1978).

$$k = k_0 * \theta_S^{Sal} * \theta_I^{Int} * \theta_T^{(Temp-20)} \quad (5)$$

Where  $k_0$  is the decay rate at 20 °C and 0 ‰ salinity,  $\theta_T$  is the decay rate from temperature deviation from 20 °C and  $Temp$  is the water temperature,  $\theta_I$  is the contribution from light intensity,  $Int$  is the light intensity in kW/m<sup>2</sup> integrated over depth,  $\theta_S$  is the contribution to the decay rate due to salinity,  $Sal$  is the salinity in ‰. For modeling objects consisting of freshwater such as this case, the salinity parameter however, has insignificant impact and was therefore not included. Moreover, the coefficient for the light intensity was neglected due to high uncertainty in what value that should be used. The temperature constant ( $\theta_T$ ) was set to 1.03.  $k_0$ , which is the decay rate at 20 °C and salinity of 0 ‰, was set to 0.24. The values of the constants were set in compliance with literature (Sokolova, 2011) and are summarized in Table 5.

Table 5 Table displaying the assigned values for constants describing the fate of the two organisms *E. coli* and Norovirus.

	$k_0$	$\theta_I$	$\theta_T$
<i>E. coli</i>	0.24	1.00	1.03
Norovirus	1	-	-

**Scenario 1** Release of untreated wastewater from Fjellfoten WWTP (Fjellfoten) during the entire modeled period 2011

The scenario is of interest since release of untreated wastewater for long periods of time occurs frequently in different WWTPs due to reconstruction or malfunction. Furthermore, The WWTP in Fjellfoten is subject for reconstruction in 2012 and the entire water volume is going to be released almost untreated for 6 months. However, the scenario is still to be considered as hypothetical since it is modeled for 2011 and input data regarding concentrations have been obtained from literature.

In the model, the yearly average discharge from Fjellfoten WWTP 0.032 m<sup>3</sup>/s was used as a constant value with constant concentrations of norovirus and E.coli. The concentration of norovirus in untreated wastewater is approximately in the span 10-50 norovirus/100ml (Håkonsen, 2012). The highest concentration in the span 50 norovirus/100ml was used in the model to simulate the worst case in the given span. For *E. coli*, the abundance in untreated wastewater is approximately 10<sup>7</sup> E.coli/100ml (Henze, 2002), which was used as concentration of *E. coli* for the whole simulated period (Table 6).

To evaluate the potential risk that a long term overflow in Fjellfoten WWTP poses on the drinking water intake, the modeled concentrations at the drinking water intake were compared to threshold values for *E.coli* in raw water. The Swedish Water and Wastewater Association have put up guideline values for safe drinking water and state 500 *E. coli*/ 100 ml as the upper threshold value for raw water (Swedish Water and Wastewater association, 2008). For the drinking water treatment plant in Gothenburg, the threshold is 400 *E. coli*/ 100 ml as the threshold for when the raw water intake in the river Göta Älv is closed (Hedström, Jönsson, & Mäki, 2009). For norovirus no such threshold values exists to be compared with.

Since oscillations occurred in some of the early runs which could have originated from instability in the numerical model, different time steps were tested to analyze the impact of the length of the time step. The time step 10 minutes was used for the main simulation. For periods which showed oscillations a time step of 1 second was tested.

**Scenario 2** *Pulse releases of untreated wastewater from Fjellfoten WWTP*

Overflow due to heavy precipitation occurs on regular basis in WWTPs where untreated wastewater is released. The aim of the simulation is to compare overflows that last for 3h and 6h respectively with continuous overflow. The average released volume of 0.032 m<sup>3</sup>/s was used together with a time series for the concentration of the affluent water. For 3h and 6h respectively E.coli concentrations of untreated wastewater was used. The concentrations were 10<sup>4</sup> E.coli/100ml for the treated water and 10<sup>7</sup> E.coli/100ml for the untreated overflowing wastewater (Henze, 2002) (

Table 6). Other parameters such as dispersion of the contamination and retention times in the system were also briefly analyzed.

*Table 6 Table summarizing the concentration of the water flow discharged from the WWTPs.*

<b>Microbe</b>	<b>Assigned value [no/100ml]</b>	<b>Reference</b>
Norovirus (Untreated wastewater)	50	(Hewitt, 2011) and (Håkonsen, 2012)
<i>E. coli</i> (Untreated wastewater)	10 <sup>7</sup>	(Henze, 2002)
<i>E. coli</i> (Treated wastewater)	10 <sup>4</sup>	(Henze, 2002)

**Validation of the microbiological modeling**

Due to lack data for the microbiological modeling, the scenarios have not been quantitatively validated.

## 4 Results

The first part of the results chapter presents the results from the validation of the mesh and hydrodynamic modeling. Subsequently, the second part contains results from hypothetical microbiological scenarios that have been simulated.

### 4.1 Mesh validation results

The comparisons between mean bathymetry value of the mesh and the measured bathymetry are presented in Table 7 below. In Figure 13 the location and extent of the compared sections are presented.

The output in mean elevation from the simulated cross sections corresponds well towards measured cross sections (Table 7). The difference in mean value in between all the eight sections is never more than 0.3 m.

*Table 7 mean bathymetry values from the mesh are compared with mean bathymetry values depth charts. Values are in meters above sea level (m.a.s.l).*

<b>Section</b>	<b>Mesh bathymetry area mean value [m.a.s.l]</b>	<b>Measured bathymetry area mean value [m.a.s.l]</b>
1	115	114.8
2	114.2	113.9
3	114.5	114.3
4	115.6	115.5
5	115.3	115.3
6	114.4	114.2
7	97.8	97.7
8	96.8	96.7

## 4.2 Sensitivity to parameter values

### 4.2.1 Sensitivity to bed roughness

The output from the sensitivity analysis is presented separately for each part of the river. The graphs of the simulated water levels are ordered as the legend, meaning that the uppermost line represents the bed roughness 1 m and the lowest represents the bed roughness 0.1 m. The dotted line represents the measured values of the water level.

#### Part 1

The resulting water levels are significantly dependent on the value of bed roughness (Figure 20). Higher values of bed roughness result in higher water level and similarly lower values result in lower water level and the dependence seems to be linear. However, during periods of high water flows the difference is bigger. During the highest water flow, the water level differs 0.9 m between the highest and the lowest bed roughness. During normal flow the water level differs in the span 0.2 to 0.45 m.

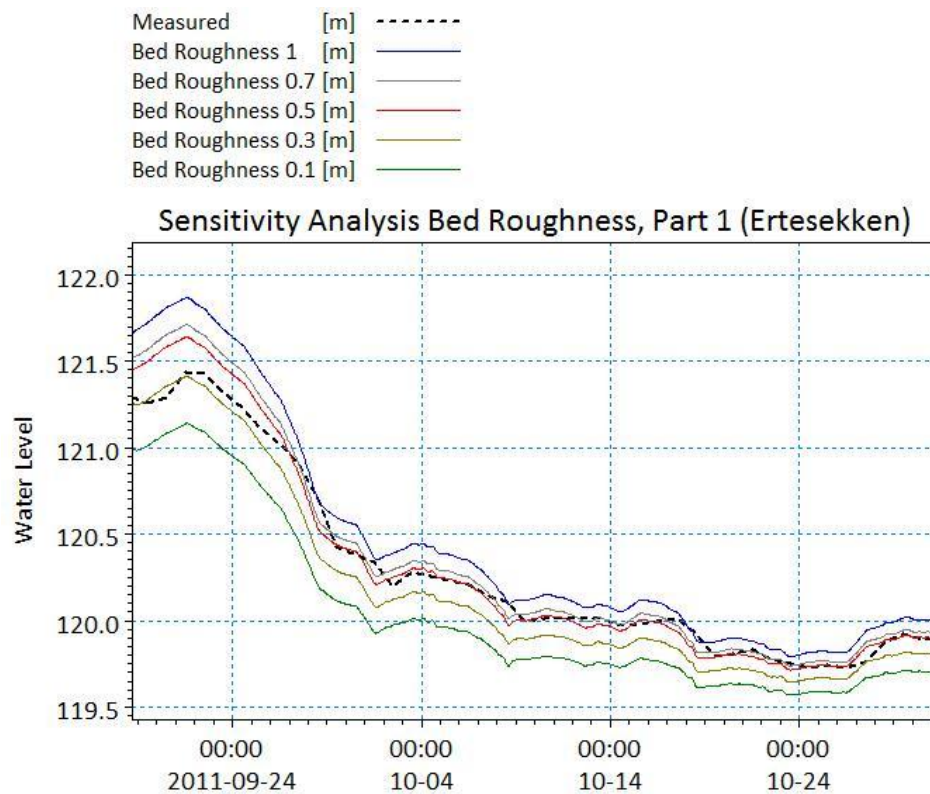


Figure 20 Sensitivity analysis performed on part 1. The dotted line represents the measured water level, while the other five lines each represent a simulated bed roughness.

## Part 2

The bed roughness influence on part 2 follows the same pattern as for part 1 where higher bed roughness yields higher water levels. However, for part 2 the spread in water levels resulting from the different values of bed roughness is generally smaller (Figure 21). The water level span between the highest and the lowest bed roughness during the simulated time period reaches from 0.05 m to 0.9.

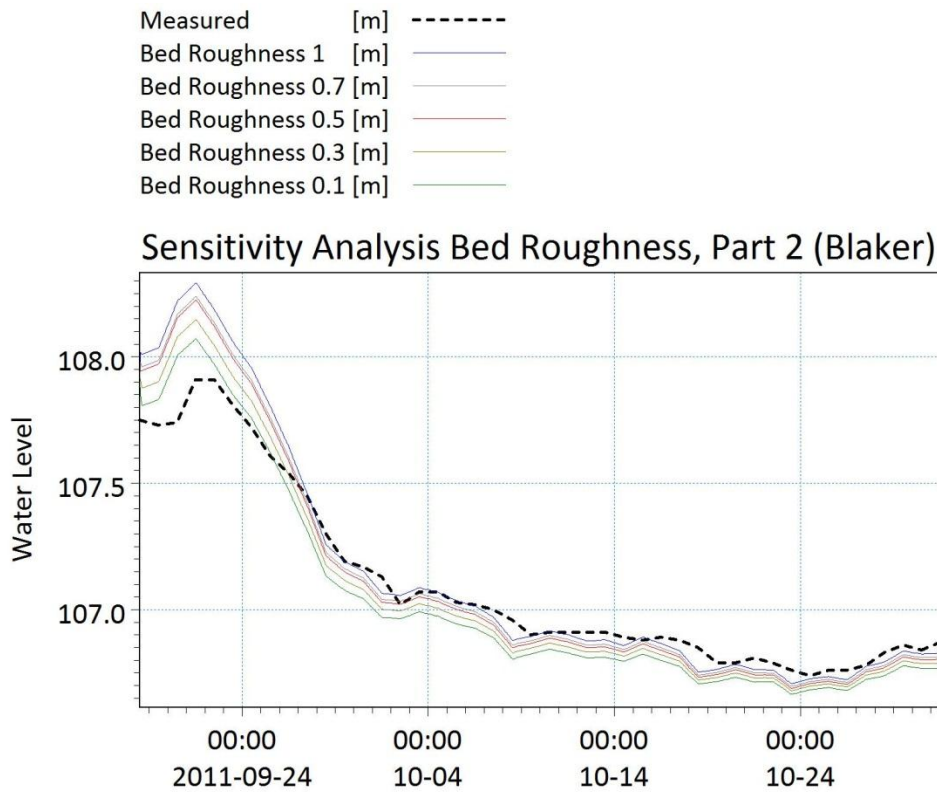


Figure 21 Sensitivity analysis performed on part 1. The dotted line represents the measured water level, while the other five lines each represent a simulated bed roughness.

### Part 3

The result from the sensitivity analysis on part 3 is displayed in Figure 22. The water level span, comparing the highest and lowest bed roughness during the simulated time period stretches from approximately 0.2 to 0.4 m.

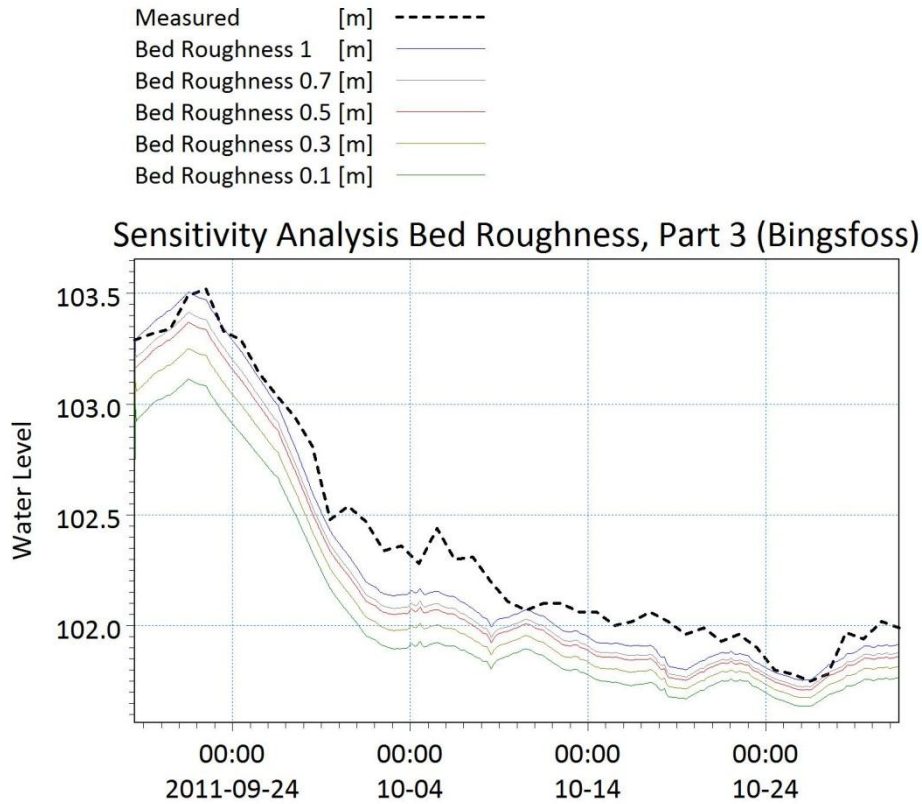


Figure 22 Sensitivity analysis performed on part 3. The dotted line represents the measured water level, while the other five lines each represent a simulated bed roughness.

## 4.2.2 Sensitivity to wind

Table 8 presents water velocities and water levels due to wind forcing. Overall, the order of magnitude of the wind forcing's influence, is a few centimeters for the water levels and a few millimeters per second for the water velocity.

However, tendencies can still be observed from the results. When the wind is running in the same direction as the water flow the top layer flows faster and the bottom one slower. The depth averaged velocity increases. Moreover, the wind results in decreased water levels in the upper part of the river stretch and increased water levels further down.

*Table 8 water velocities and water levels due to wind forcing.*

	No wind	Wind (10 m/s, 20° from north)	Difference due to wind
Velocity in top layer [m/s]	0.453	0.458	0.005
Velocity in bottom layer [m/s]	0.334	0.327	-0.007
Depth averaged velocity [m/s]	0.452	0.459	0.007
Water level upper boundary [m]	107.164	107.15	-0.014
Water level middle part [m]	106.825	106.829	0.004
Water level lower boundary [m]	106.523	106.523	0

## 4.3 Hydrodynamic validation results

### 4.3.1 Water level

All data that were not used as input data at the boundaries were used for validation of the hydrodynamics. Overall the simulated results for the validation points on all parts of the river correspond well with the measured data. The comparison between simulation output and measured data is presented in Figure 23 - Figure 30 along with small maps that display the locations of validation points.

#### Part 1

The highest differences in water levels between modeling results and measured data, at the validation points in Funnefoss and Ertesekken (Figure 7), occur in the beginning of the simulation period during the maximum flow. The difference is 0.45 m for Funnefoss (Figure 23) and 0.3 m for Ertesekken (Figure 24) respectively.

From mid-October to the end of the simulation period, when average flows occur, the graphs correspond well. During this period the differences between measured and modeled water levels ranges from 0 to 10 cm.

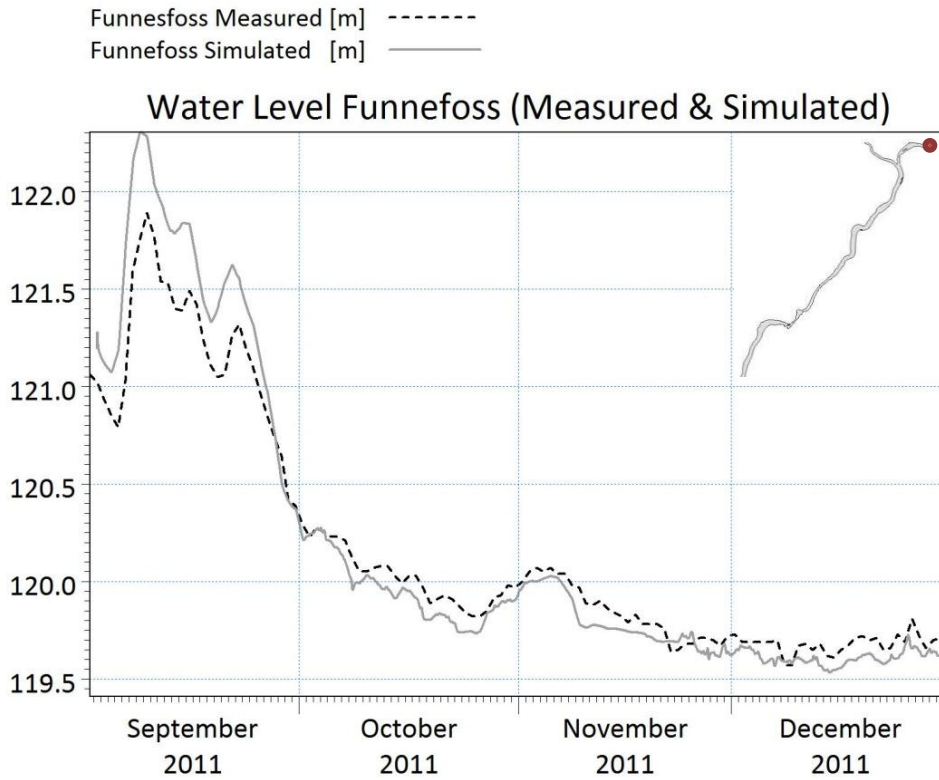


Figure 23 Measured and simulated water level at Funnefoss. The dot on the map in the right corner displays the location of the validation point.

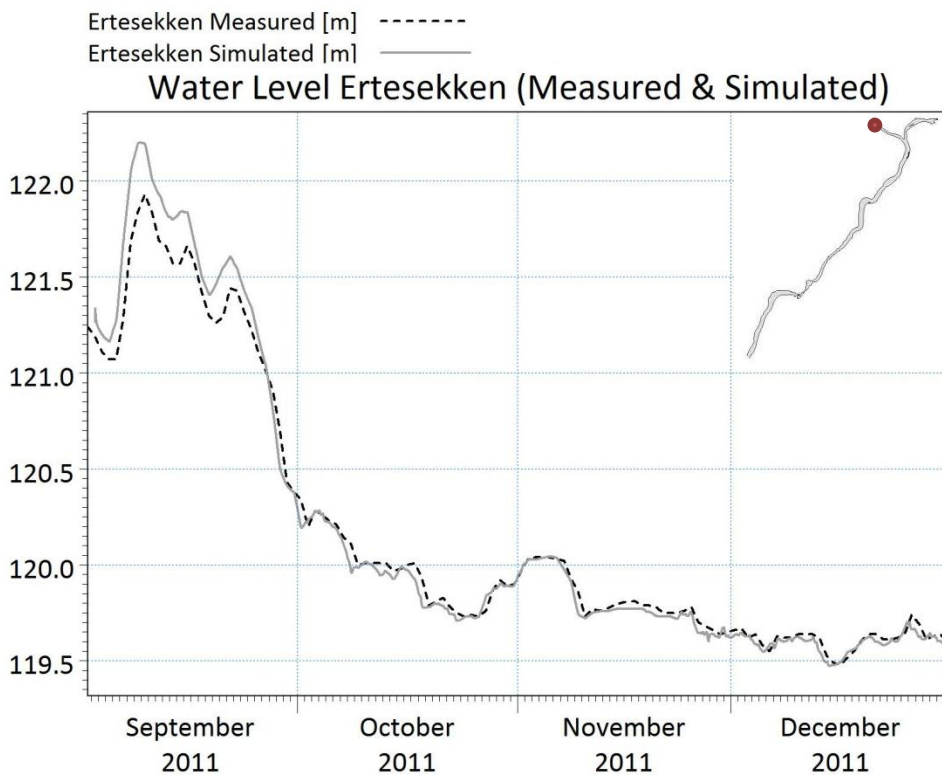


Figure 24 Measured and simulated water level at Ertesekken. The dot on the map in the right corner displays the location of the validation point.

## Part 2

The validation point at Rånåsfoss (Figure 25) lacks measured data for the period from 2011-09-01 to 2011-10-21. During the remaining period the two graphs relates well.

The water level at Blaker (Figure 26) follows the same patterns as for the validation points at part 1. Simulated water levels are higher than the measured water levels at high flows in the beginning of the simulated period and fit better in the end of the period when lower flows occur. The maximum difference is 0.5 m which occurs during the peak flow and the difference for the period 2011-10-01 to 2011-12-31 reaches from 2 to 10 cm.

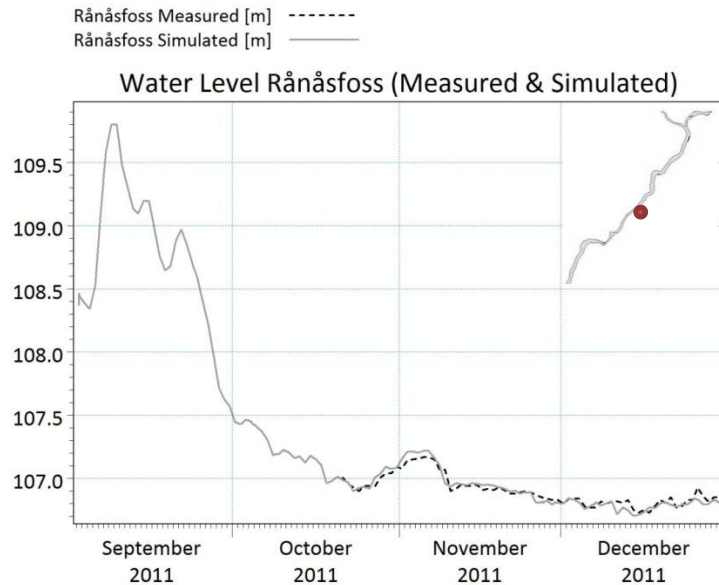


Figure 25 Measured and simulated water level at Rånåsfoss. The dot on the map in the right corner displays the location of the validation point.

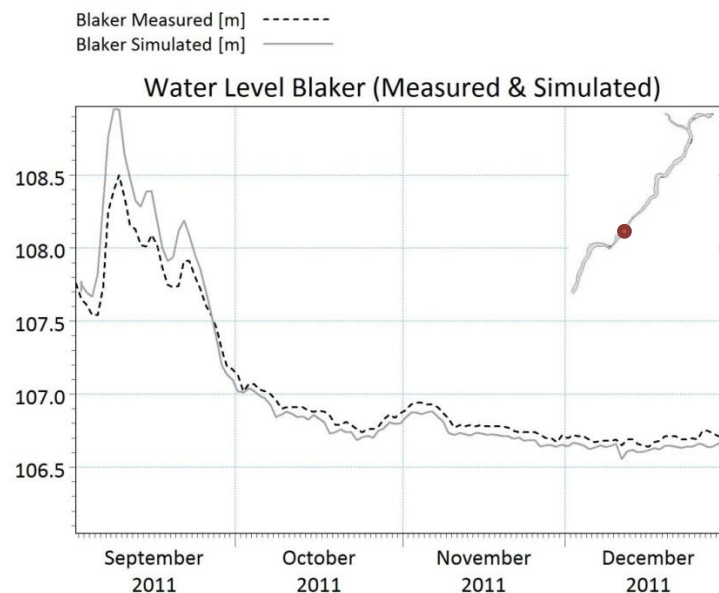


Figure 26 Measured and simulated water level at Blaker. The dot on the map in the right corner displays the location of the validation point.

### Part 3

The validation point at Bingsfoss (Figure 27) diverges from the pattern on part 1 and part 2. The highest level difference at Bingsfoss occurs during the period with average flows in contrast to the previous comparisons. The differences for the last three months vary from 0 to 15 cm.

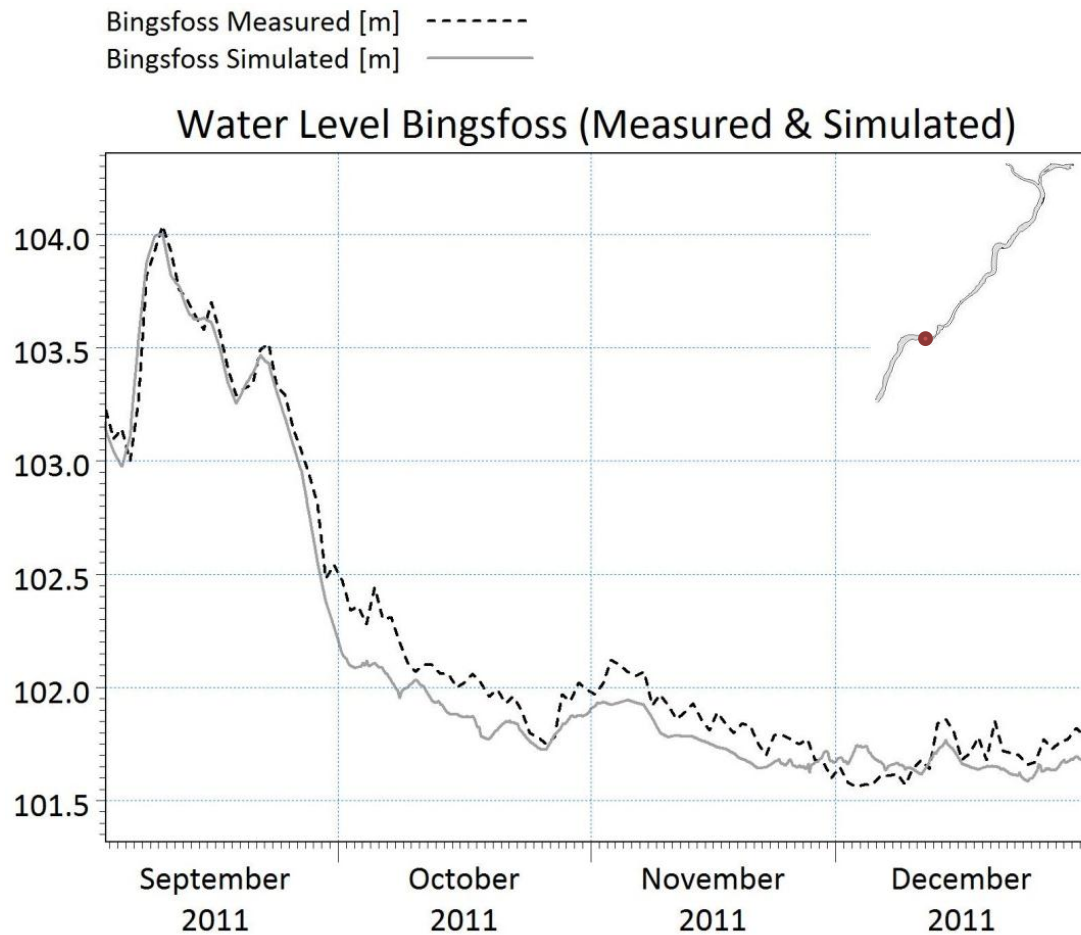


Figure 27 Measured and simulated water level at Bingsfoss. The dot on the map in the right corner displays the location of the validation point.

### 4.3.2 Velocity

The measured velocity in Blaker corresponds well to the simulated velocities. In Figure 28 the water velocity in three mesh elements adjacent to the monitoring station is compared to the measured values.

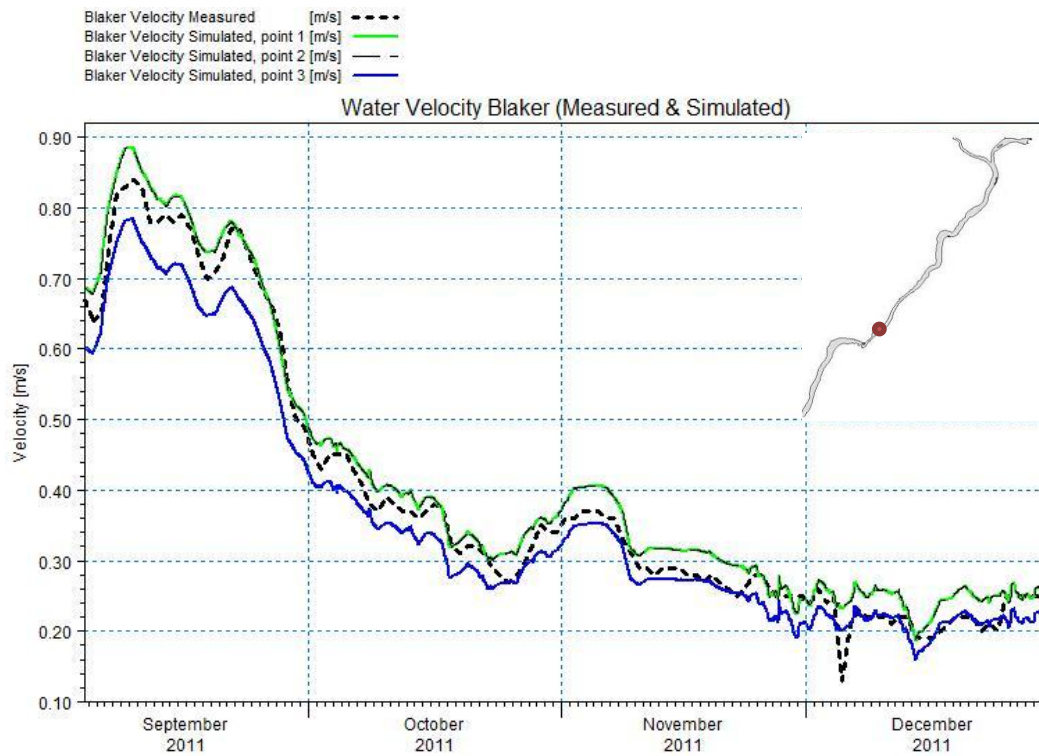


Figure 28 Measured and simulated velocities in Blaker. The simulated values are obtained from three different mesh elements adjacent to the location of the monitoring station.

Over a cross section, the velocities are distributed as expected, with lower velocities close to the river bed and higher velocities in the inner part of the stream Figure 29.

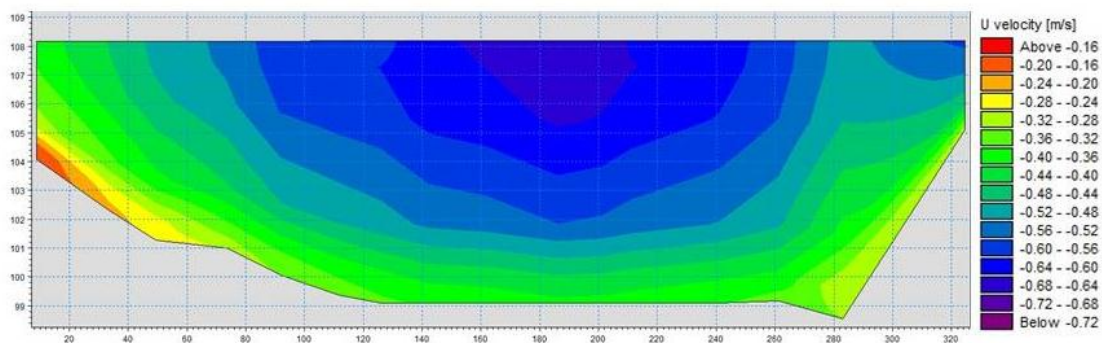


Figure 29 Modeling results regarding water velocities in a cross section. The water flow in the section is directed towards south west and the figure illustrates the velocity component in east-west direction ( $U$  velocity). In the figure, the water flow is directed towards the reader.

### 4.3.3 Comparison to aerial photos

In Figure 30, left, the modeled concentration of an arbitrary diluted substance is visualized and the model shows behavior of slow mixing of water. The west river branch is given a different concentration than the east branch in order to analyze the

mixing after the river fork. The turbulence of the modeled flow is low and the concentration gradient only vanishes slowly. In Figure 30, right, the aerial photo also suggests that the mixing of water from the two branches is slow since a gradient in turbidity can be observed throughout the stretch.

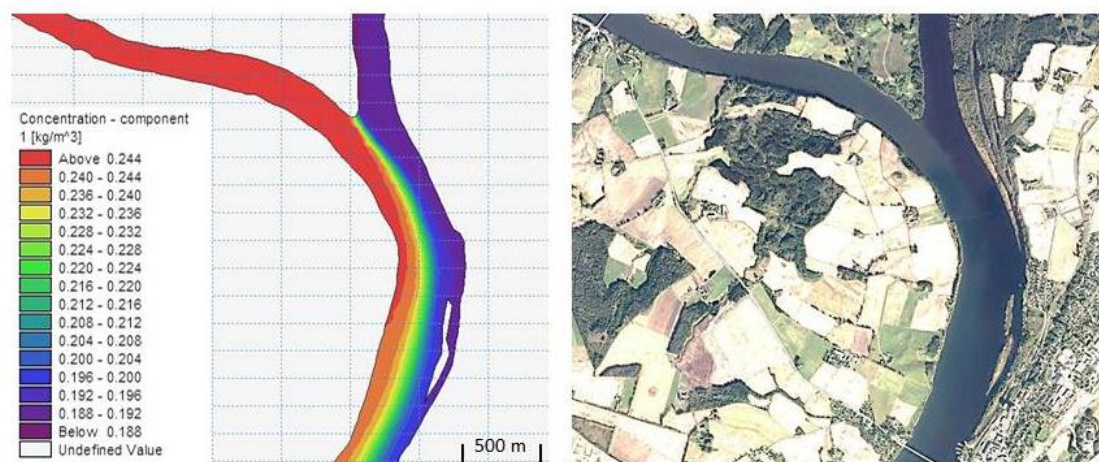


Figure 30 left: modeled mixing downstream the river fork when water with different concentration merge. The gradient only vanishes slowly. Right: aerial photo showing water with different turbidity merge in the river fork. Likewise, the mixing occurs slowly and the gradient can be observed throughout the stretch.

The statement that the water of the connecting rivers mixes slowly due to low turbulence was further strengthened by Björn-Dag Gundersen, head of information at Akershus Energi AS in an interview. He has lived by the river Glomma all his life and reports that when swimming across the river in the summer, a distinct border between water with different temperatures is often experienced, sometimes even 10 km downstream the fork (Gundersen, 2012).

Even though neither the aerial photo nor the interview validates the simulated mixing processes of the model, they nevertheless provide an indication of compliance between the model and the reality.

## 4.4 Output from microbial simulation of scenarios

### Scenario 1

The resulting concentrations *E.coli* and norovirus are presented in Figure 31 along with the water flow as a reference. Furthermore, the figure presents the guideline and threshold values of the Swedish Water and Wastewater Association and Göteborg Vatten. The modeled concentration of *E.coli* exceeds the threshold value 400 *E.coli*/100ml used by Göteborg Vatten for the major part of the modeled period. Furthermore, the concentration exceeds the guideline value 500 *E.coli*/100ml used by the Swedish Water and Wastewater Association for a significant part of the period. For norovirus, the resulting concentrations are presented in Figure 32.

The result from the additional simulation with a 1 second time step performed on the period 27<sup>th</sup> -30<sup>th</sup> of November is displayed in Figure 33. As can be seen in figure, the oscillations of the graph are disappeared when using a time step of 1 second instead of 10 minutes.

The contamination plume and the dilution of the discharged wastewater are presented in Figure 34. It can be seen how the concentration at the uppermost cross section is more concentrated to a specific part of the river. At cross section 2 and 3 the plume is more diluted and the concentration differences over the cross sections are more evenly distributed. However, there are still horizontal and vertical gradients over cross section 3.

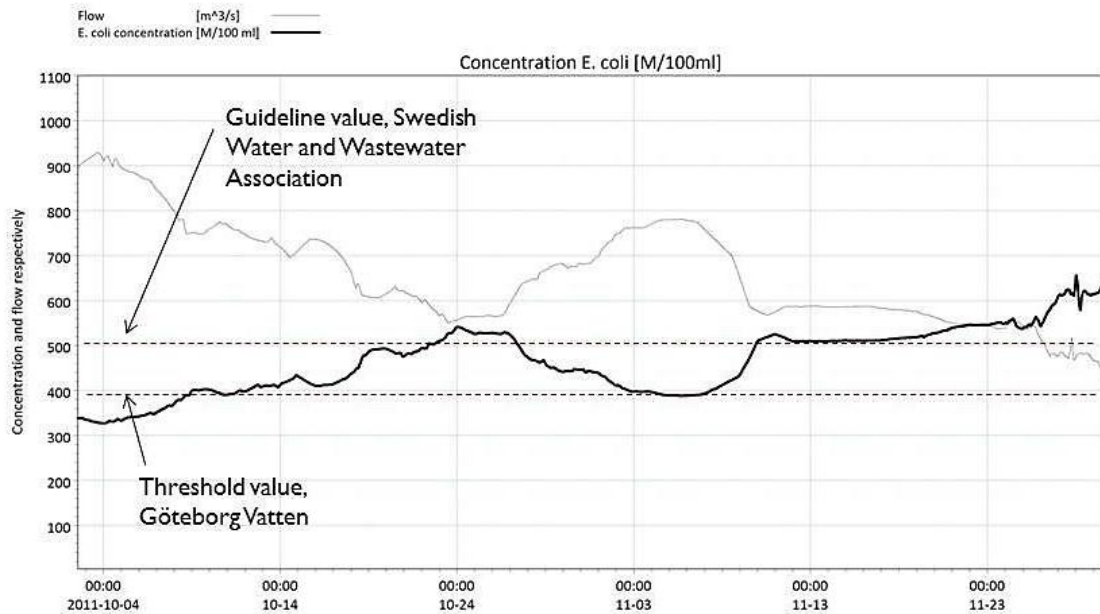


Figure 31 resulting mean concentrations of *E.coli* in Rånåsfoss over a cross section. The flow of the river is also presented in the figure as a reference and it can be seen that the concentration is inversely proportional to the flow due to a constant release of *E.coli*. Furthermore, guideline and threshold values of the Swedish Water and Wastewater

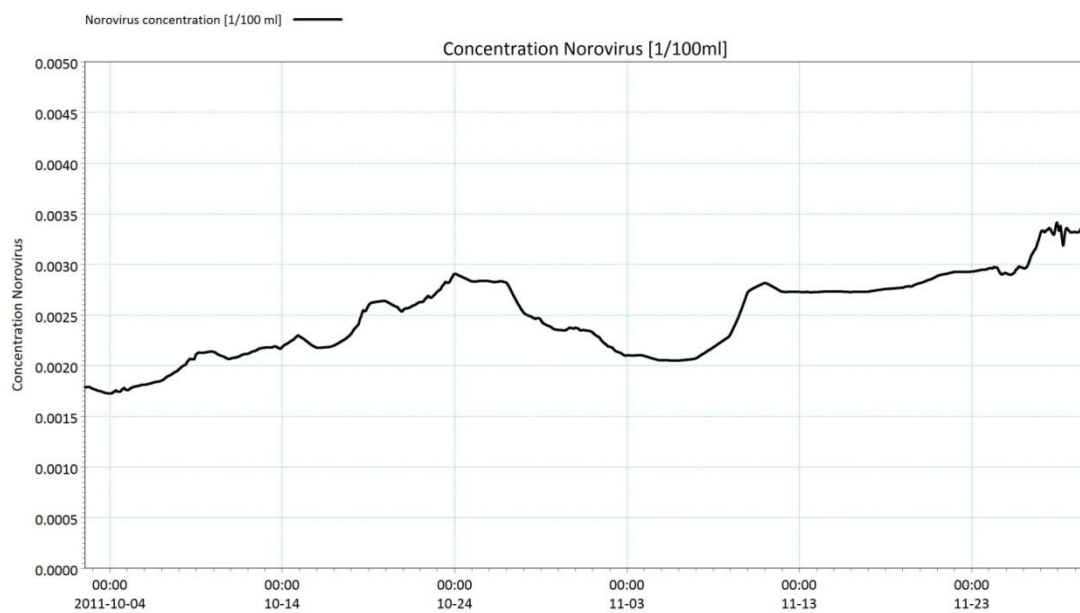


Figure 32 resulting mean concentrations of norovirus in Rånåsfoss over a cross section. From the shape of the graph it can be seen that the concentration is inversely proportional to the water flow in the river which is displayed in

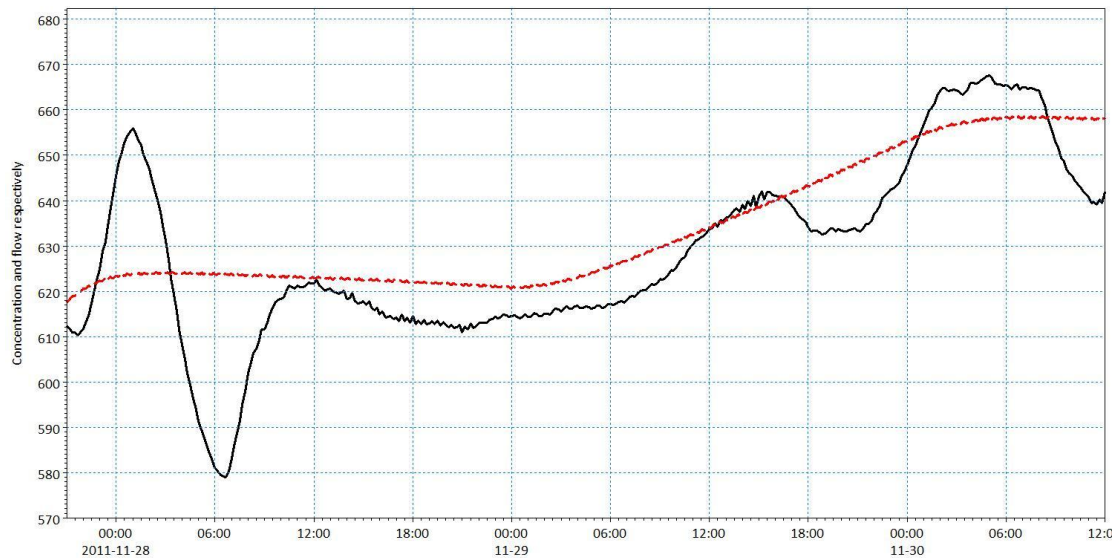


Figure 33 Graph displaying the difference in oscillations between the simulations made with a 10 minute time step and 1 second. The black line is the concentration when using a 10 minutes time step. The concentration is given in *E. coli*/100ml

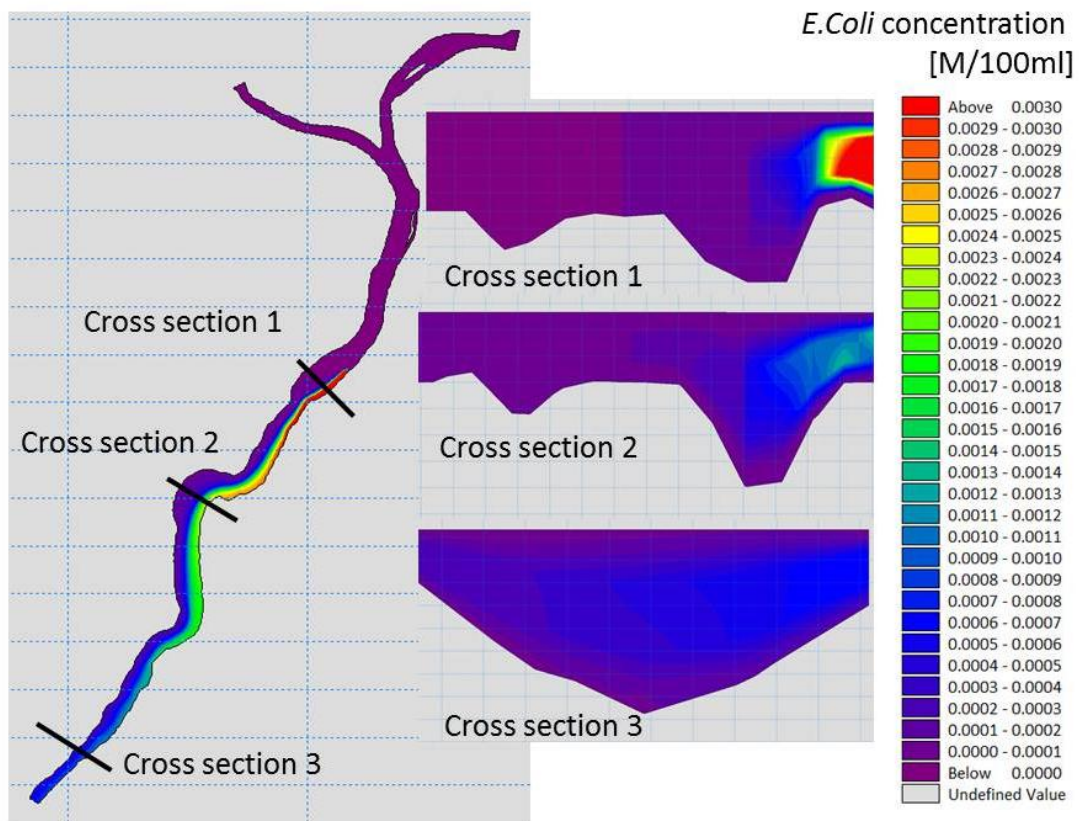


Figure 34 the contamination plume from the discharge of untreated wastewater in Fjellfoten from above and in three cross sections.

## Scenario 2

Figure 35 displays a pulse release of untreated wastewater discharged from Fjellfoten and the resulting concentrations in three different cross sections downstream. The presented concentrations are averaged over the cross sections and are located below Fjellfoten WWTP, at Rånåsfoss and at the raw water intake. The top concentration in the released pulse of discharged water decreases with the travelling time. In addition, the duration of the pulse increases with the travelling time. For the release with the duration of 6h higher concentrations are reached than for the release of 3h. At the raw water intake, the 3h pulse affect the water quality for 12h and the 6h release affects the concentration at the intake for 18h.

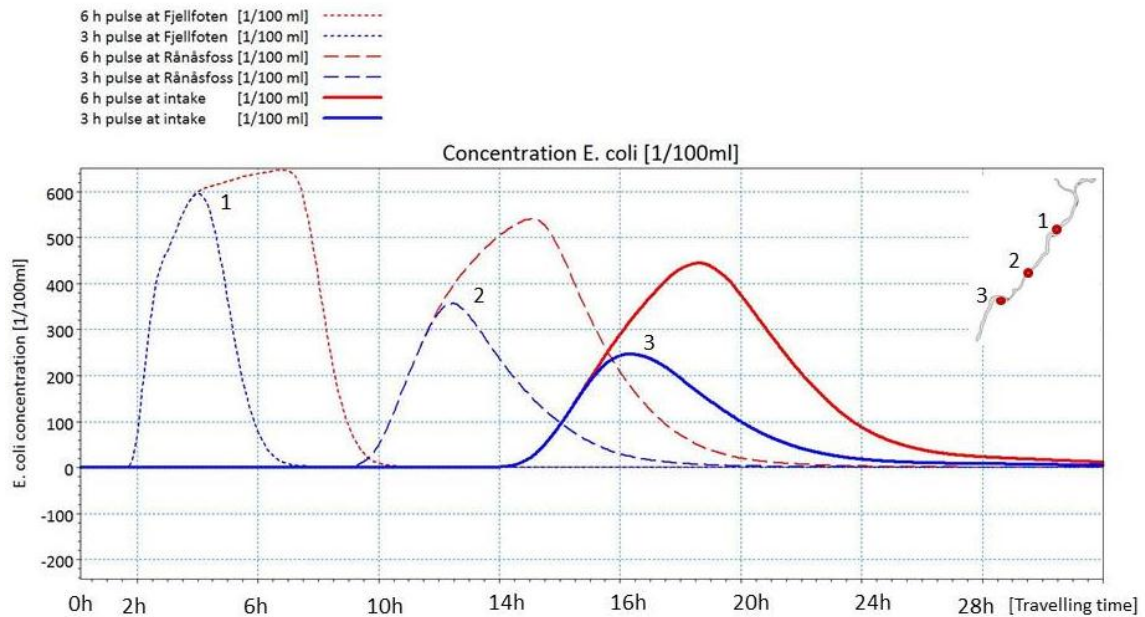


Figure 35 A pulse of untreated wastewater being released from Fjellfoten WWTP. The resulting averaged concentrations in three cross sections are displayed. Cross section 1 is below Fjellfoten WWTP, 2 is at Rånåsfoss and 3 is at the raw water intake

## 5 Analysis and Discussion

This project has the aim to simulate the hydrodynamics and transport of norovirus and *E. coli* within the river Glomma. This was carried out by fulfilling different predefined objectives. To obtain the final result computational modeling was performed using the software MIKE by DHI, where the modeling process was conducted in three different steps: domain specification and generation of mesh, hydrodynamic simulation as well as modeling of microbial dynamics. The final result was acquired from connecting the hydrodynamic and microbiological models.

The mesh of parts 1 and 3 represents the bathymetry of the river adequately. However, since the resolution of the input data (1 m equidistant) is much greater than the elements of the used mesh, much information regarding the bathymetry is lost when generating the mesh. For part 2, where the bathymetry data were collected in a field survey, the bathymetry is connected to significant uncertainties since a substantial part of the bathymetry values have been interpolated. Moreover, the eco sounder that was used is also a potential source of uncertainty.

The hydrodynamic simulations of the river Glomma seems to represent the reality satisfactory since the outputs from the simulations correspond well to measured water level and velocity data. However, the simulated water levels tend to be higher than the measured ones during high water flows in the river and lower than the measured ones during low flows. A possible explanation of these discrepancies is the simplification of the river cross section made in the mesh generation. In the model, the land-water boundary is fixed and specified from the mean water level in the river. In the reality however, the surface area of the river expands during high water flows as the water inundates the shore. Since the shoreline in the model is fixed, a difference in cross section area can therefore only be achieved by increasing or decreasing the water level, this results in greater fluctuations of the water level in the model than in reality. Since the model was calibrated and validated for average water flow, it is probably most adapt for modeling normal water flows.

The properties of water mixing in the river are crucial when modeling spread of pathogens. For example it is of great importance to know the distance a point release has to surge before its concentration is homogenous over the cross section. An estimation of such properties was acquired from the model but no validation has been done quantitatively. The distance before the concentration is homogenous over the cross section is probably dependent on a number of different parameters affecting for example the density and turbulence of the water, such as water temperature and flow. An attempt to validate the mixing behavior of the river quantitatively would therefore be both costly and difficult since many different conditions would need to be explored.

In the modeling of norovirus a constant concentration was used for the absence of norovirus in the untreated wastewater. As mentioned earlier, this is not the case in the reality where the concentrations vary with the season. An interesting period of time to model in regard to virus spreading is the first quarter of 2011 since the concentrations are often the highest during the winter months (SMI, 2012). Due to shortage of validation data for the hydrodynamics and to lack of time in some extent, this was not done. However, since the hydrodynamic model has been calibrated and validated for the fourth quarter of 2011 where validation data were accessible, a theory is that the model could be used for any period of time with similar hydrologic conditions.

The modeled concentrations of *E.coli* and norovirus were oscillating slightly from 2011-11-23 and forth when the time step was set to 10 minutes. A theory to why this phenomenon occurs is that the CFL-condition was not met and the time step was too long in comparison to the smallest cell size and the water velocity. This could then have caused numerical instability. The theory is strengthened by the fact that the oscillations disappeared when the time step was reduced to 1 second. However, performing simulations over long periods of time with 1 second time steps is very computationally expensive. If the computational capacity needed does not exist, either the grid size has to be increased or the oscillations put up with. Oscillations that occurred for the 10 minute time step reached a few percent of the result value, with the mean value of the result unaffected.

In the simulation of scenario 1 the presented guidelines and thresholds were exceeded in regard to *E.coli*. This implies that a long term release of untreated wastewater in Fjellfoten WWTP would pose a noteworthy risk to the drinking water quality of the drinking water treatment plant downstream. However, what should be kept in mind is that the *E.coli* concentration of untreated wastewater was set to a constant obtained from literature. Furthermore, extent of dilution of a contamination in the river is determined by the water flow.

In scenario 2, it was shown that the duration of a release is of importance to the resulting concentrations at the raw water intake. For a release with the duration of 3h, the water quality at the raw water intake is affected for 12h and reaches the maximum concentration of approximately 250 *E. coli*/100ml. Similarly, for the 6h release the water quality at the intake is affected for 18h reaching a maximum concentration of approximately 450 *E. coli*/100ml. Hence, a release with longer duration results in higher concentrations given that the concentration of the release is constant.

Since detection of viruses is complicated and difficult with existing techniques the uncertainties in the measurements are often high (SMI, 2012). It is therefore problematic to perform a validation of the microbiological model that is statistically significant.

Even though computational models are supposed to exemplify the reality, the model output does often not correspond well with the real world. Reliance in a poor model might be deceiving and it is therefore essential to validate the model in order to evaluate how well it corresponds with the reality. However, even though a model is validated and corresponds well to the reality, the results always hold uncertainties. One source of uncertainty may be the input data, and the quality of a model output is never higher than the quality of the input.

## 6 Areas of further investigation

Since the outcome of the model is to be used further on in the VISK project as input to a QMRA, it is important that the model is as accurate as possible which can be achieved through further investigation.

In order to validate the hydrodynamic model further, additional time series of velocity and water level would be needed. The model could at best be validated for time periods which are independent of the time period used for the calibration. At the performed validation, parts of the period did overlap but the bigger part did not. Moreover, since the model is three-dimensional a validation in three dimensions should be carried out. The validation could be done by the release of a tracer, for example rhodamine, where the concentration would be measured in multiple points downstream. Another way could be to measure the conductivity in multiple points downstream the WWTP.

Furthermore, additional data are needed for validation of the microbiological model. If possible, time series measurements of concentrations would be needed at the raw water intake, in the water discharged from the WWTP and in the untreated wastewater. Moreover, the accuracy of the measurements would have to be relatively high in order to get a significant correspondence. In addition, a more thorough analysis of the fate of different pathogens should be coupled to the hydrodynamic model in order to better describe the spread.

It is also suggested that a sensitivity analysis is carried out more thoroughly of which parameters that model is most sensitive to. This could for example be done statistically by Monte Carlo simulation.

Finally, the models sensitivity to the grid size should also be analyzed since higher mesh resolution often yield more accurate results (Legrand, Deleersnijder, Hanert, Legat, & Wolanski, 2006). If shown that a different mesh resolution would yield different results, simulations should be done with higher resolution of the computational mesh. However, this would imply increased run times for the simulations. More powerful machines are recommended for the task or even use of high performance computer labs. Since depth data are available for most parts of the modeled stretch with 1 m resolution the potential of refining the mesh is extensive.

## 7 Conclusion

The approach with coupled hydrodynamic and microbiological models is well suited for predicting pathogen concentrations in drinking water sources. The approach is especially appropriate for modeling pathogens which are difficult to detect and which are not well represented by microbial indicators. Furthermore, models are well suited for generating input concentrations for QMRA analysis.

Coupled hydrodynamic microbiological models can be used to analyze hypothetical scenarios and future events that are more or less likely to happen. Since the approach grasps the whole system, from WWTP to drinking water source it can be used as a tool for establishing guidelines and regulation for waste water discharge.

It is important to keep in mind that models are only an attempt to represent the reality and the results hold many uncertainties. Validation of the models is therefore crucial.

The hypothetical scenarios simulated show clear tendencies that overflows are likely to affect the water quality at the raw water intake. A overflow where all water in Fjellfoten WWTP is released untreated implies that threshold values regarding safe drinking water at the raw water intake will be exceeded.

The flow of the river is of high importance both regarding the transportation time and the dilution of the fecal contaminant.

## 8 Bibliography

- Aasand, F. I. (2011, 8 16). *Norsk Vann*. Retrieved 05 18, 2012, from <http://www.norskvann.no/component/content/article/69-prosjekter/aktive/prosjekter-samfunn/95-klimatilpasningstiltak-i-va-sektoren>
- Ahmed, R. (2004). *Numerical Schemes Applied to the Burgers and Buckley-Leverett Equations*. University of Reading.
- Akershus Energi AS. (2012). *Akershus Energi*. Retrieved 03 22, 2012, from <http://www.aeas.no/>
- Andersson, B. (2009). *Computational Fluid Dynamics for Chemical Engineers*. Gothenburg.
- Asplan Viak. (2012). *Årsrapport Rånåsfoss 2011*. Sörum: Asplan Viak.
- Chow, C. (1959). *Open-Channel Hydraulics*. Singapore: McGraw-Hill Book Co.
- Cloete, T. E. (2004). *Microbial waterborne pathogens*. London: IWA publishing.
- Courant, R., Friedrichs, K., & Lewy, H. (1967). On the Partial Difference Equations of Mathematical Physics. *IBM*, 215-234.
- DHI. (2011). *ECO LAB (Short Scientific Description)*. Horsholm, Denmark: MIKE by DHI.
- DHI. (2011). *ECO LAB (User Guide)*. Horsholm, Denmark: MIKE by DHI.
- DHI. (2011). *MIKE 21 & MIKE 3 Flow Model FM Scientific Documentation*. Horsholm, Denmark: MIKE by DHI.
- DHI. (2011). *MIKE 3 Flow Model FM, Hydrodynamic Module*. Horsholm, Denmark: MIKE by DHI.
- DHI. (2011). *MIKE 3 Flow Model FM, Hydrodynamic Module*. Horsholm, Denmark: MIKE by DHI.
- DHI. (2011). *MIKE Zero Preprocessing and Postprocessing*. Horsholm, Denmark: MIKE by DHI.
- DHI. (2011). *MIKE ZERO: Creating 2D Bathymetries*. Horsholm, Denmark: MIKE by DHI.
- DHI. (2011). *Water Quality WQ Template, ECO Lab (Scientific Description)*. Horsholm, Denmark: MIKE by DHI.
- Eriksson, C. (2012, 04 20). Project manager, fil dr. oceanography. (J. Senning, Interviewer)
- GLB, (Glommens och Laagens Brukserierforening). (2011). *Årsrapport 2010*. Lilleström: Glommens och Laagens Brukserierforening.
- Gundersen, B. D. (2012, 05 07). Head of information at Akershus Energi AS.
- Häfliger, D., Hübner, P., & Lüthy, J. (2000). Outbreak of viral gastroenteritis due to sewage-contaminated drinking water. *International Journal of Food Microbiology*, 123-126.
- Hägström, S. (2009). *Hydraulik för samhällsbyggnad*. Stockholm: Liber AB.

- Håkonsen, T. (2012, 05 18). Consultant. (A. Emanuelsson, Interviewer)
- Harwood, V., Levine, A., Scott, T., Chivukula, V., Lukasik, J., Farrah, S. R., et al. (2005). Validity of the Indicator Organism Paradigm for Pathogen Reduction in Reclaimed Water and Public Health Protection. *Applied Environmental Microbiology*, 3163–3170.
- Hedström, A., Jönsson, R., & Mäki, A. (2009). *Early warning system - Is this something for our municipality?* Stockholm: Svenskt Vatten AB.
- Henze, M. (2002). *Wastewater Treatment*. Berlin: Springer-Verlag Berlin and Heidelberg GmbH & Co. K.
- Herzog, A. B., Bhaduri, P., Stedtfeld, R., Gregoire, S., & Farhan, A. (2010). Detection and Occurrence of Indicator Organisms and Pathogens. *Water Environment Research*, 883-907.
- Hewitt, J. (2011). Influence of wastewater treatment process and the population size on human virus profiles in wastewater. *Water Research*, 6267-6276.
- InterReg. (2012). *InterReg*. Retrieved 05 18, 2012, from <http://interreg.tillvaxtverket.se/europeiskterritoriellttsamarbete/gransregionalasamarbetsprogram/oresundkatttegatskagerrak.4.62577d6e125504a77e0800035632.html>
- IPCC. (2007). *IPCC Fourth Assessment Report: Climate Change 2007*. Cambridge: IPCC.
- Kukkula, M., & Arstila, P. (1997). Waterborne Outbreak of Viral Gastroenteritis. *Scandinavian Journal of Infectious Diseases*, 415-418.
- L'Abée-Lund, J. H., Eie, J. A., Faugli, P. E., Haugland, S., Hvidsten, N. A., Jensen, A. J., et al. (2009). *Rivers of the boreal uplands*. Elsevier Ltd.
- Legrand, S., Deleersnijder, E., Hanert, E., Legat, V., & Wolanski, E. (2006). High-resolution, unstructured meshes for hydrodynamic models of the Great Barrier Reef, Australia. *Estuarine, Coastal and Shelf Science*, 36-46.
- Lindhe, A. (2008). *Integrated and probabilistic risk analysis of drinking water systems*. Göteborg: Chalmers University of Technology.
- Mancini, J. (1978). Numerical Estimates of Coliform Mortality Rates under Various Conditions. *Journal of the water pollution control federation*, 2477-2484.
- Niea, L., Lindholma, O., Lindholmb, G., & Syversen, E. (2009). Impacts of climate change on urban drainage systems – a case study in Fredrikstad, Norway. *Urban Water Journal*, 323–332.
- NINA, ENRI (Norwegian Institute for Nature Research and Eastern Norway Research Institute). (2000). *The Glomma & Laagen Basin*. Cape Town: World Commission on Dams Secretariat (WCD).
- NRV & NRA, (. R. (2012). *NRV/NRVA*. Retrieved 02 10, 2012, from <http://www.nrva.no/>
- NRV, NRA (NEDRE ROMERIKE VANNVERK IKS | NEDRE ROMERIKE AVLØPSELSESKAP IKS). (2012). *NRV/NRVA*. Retrieved 02 10, 2012, from <http://www.nrva.no/>

- NVE (Norwegian Water Resources and Energy Directorate). (2012). *www.nveatlas.no*. Retrieved 2012, from NVE Atlas: <http://atlas.nve.no/ge/Viewer.aspx?Site=NVEAtlas>
- SCB. (2010). *The future population of Sweden 2010-2060*. Stockholm: Statistics Sweden.
- Sinkerud, J. (2012, 04 30). Operation technician Sorum municipality. (L. Solli Sal, Interviewer)
- SMI. (2011). *Cryptosporidium i Östersund*. Solna: Smittskyddsinstitutet.
- SMI. (2012). *Norovirus i vatten - En litteraturstudie*. Solna: Smittskyddsinstitutet.
- Sokolova. (2011). *Hydrodynamic and Microbiological Modelling of Water Quality in Drinking Water Sources*. Gothenburg: Chalmers University of Technology.
- Sokolova, E. (2011). *Hydrodynamic and Microbiological Modelling of Water Quality in Drinking Water Sources*. Gothenburg: Chalmers University of Technology.
- Sokolova, E., Åström, J., Pettersson, T. J., Bergstedt, O., & Hermansson, M. (2011). Inactivation of Bacteroidales genetic marker for microbial water quality modeling of drinking water sources. *Environmental Science and Technology*.
- Solli Sal, L. (2012, 05 16). Project Leader and Process Engineer. (J. Senning, Interviewer)
- Swedish Water and Wastewater association. (2008). *Råvattenkontroll – Krav på råvattenkvalitet*. Stockholm: Svenskt Vatten.
- Swedish Water and Wastewater Association. (2008). *Råvattenkontroll – Krav på råvattenkvalitet*. Stockholm: Svenskt Vatten.
- Tran, A. N., & Brytting, M. (2010). Dagisvirus som påverkar oss alla . *Smittskydd*, Nr. 1.
- Versteeg, H., & Malalasekera, W. (2007). *An Introduction to Computational Fluid Dynamics, The Finite Volume Method*. London: Pearson Education Limited.
- Viak Asplan. (2012). *Årsrapport Fjellfoten RA 2011*. Nes: Asplan Viak.
- VISK. (2012). *Bakgrund*. Retrieved 2012, from VISK: [www.visk.nu](http://www.visk.nu)
- WHO. (2008). *Guidelines for Drinking-water Quality*. Geneva: World Health Organization.
- WHO. (2008). *Guidelines for Drinking-water Quality*. Geneva: World Health Organization.
- WHO. (2012). Retrieved 05 10, 2012, from World Health Organisation regional office for Europe: <http://www.euro.who.int/en/what-we-do/health-topics/environment-and-health/water-and-sanitation>
- WHO. (2012). Retrieved 05 10, 2012, from World Health Organisation regional office for Europe: <http://www.euro.who.int/en/what-we-do/health-topics/environment-and-health/water-and-sanitation>